



# New evidence of glacier surges in the Central Andes of Argentina and Chile

Progress in Physical Geography

1–34

© The Author(s) 2018

Article reuse guidelines:

[sagepub.com/journals-permissions](http://sagepub.com/journals-permissions)

DOI: 10.1177/0309133318803014

[journals.sagepub.com/home/ppg](http://journals.sagepub.com/home/ppg)**Daniel Falaschi** 

Instituto Argentino de Nivología, Glaciología y Ciencias Ambientales (IANIGLA), Mendoza, Argentina

**Tobias Bolch**

University of Zurich, Zurich, Switzerland

**Maria Gabriela Lenzano**

Instituto Argentino de Nivología, Glaciología y Ciencias Ambientales (IANIGLA), Mendoza, Argentina

**Takeo Tadono**

Earth Observation Research Center (EORC), Japan Aerospace Exploration Agency (JAXA), Sengen, Tsukuba, Ibaraki, Japan

**Andrés Lo Vecchio**

Instituto Argentino de Nivología, Glaciología y Ciencias Ambientales (IANIGLA), Mendoza, Argentina

**Luis Lenzano**

Instituto Argentino de Nivología, Glaciología y Ciencias Ambientales (IANIGLA), Mendoza, Argentina

## Abstract

In contrast to the large surge-type glacier clusters widely known for several mountain ranges around the world, the presence of surging glaciers in the Andes has been historically seen as marginal. The improved availability of satellite imagery during the last years facilitates investigating of glaciers in more detail even in remote areas. The purpose of the study was therefore to revisit existing information about surge-type glaciers for the Central Andes of Argentina and Chile ( $32^{\circ} 40' - 34^{\circ} 20' S$ ), to identify and characterize possible further surge-type glaciers, providing new insights into the mass balance and evolution of the velocity of selected glaciers during the surge phase. Based on the analysis of 1962–2015 satellite imagery, historical aerial images, differencing of digital elevation models and a literature survey, we identified 21 surge-type glaciers in the study area. Eleven surge events and six possible surge-type glaciers were identified and described for the first time. The estimation of annual elevation changes of these glaciers for the 2000–2011 period, which encompasses the latest surge events in the region, showed heterogeneous behavior with strongly negative to positive surface elevation change patterns ( $-1.1$  to  $+1.0 \text{ m yr}^{-1}$ ). Additionally, we calculated maximum surface velocities of  $3 \pm 1.9 \text{ m d}^{-1}$  and  $3.1 \pm 1.1 \text{ m d}^{-1}$  for two of the glaciers during the latest identifiable surge events of 1985–1987 and 2003–2007. Within this glacier cluster, highly variable advance rates ( $0.01 - 1 \text{ km yr}^{-1}$ ) and dissimilar surface velocities at the surge peak ( $3 - 35 \text{ m d}^{-1}$ ) were

## Corresponding author:

Daniel Falaschi, Instituto Argentino de Nivología, Glaciología y Ciencias Ambientales (IANIGLA), CCT-Mendoza, Ruiz Leal s/n, Parque General San Martín, 5500 Mendoza, Argentina.

Email: [dfalaschi@mendoza-conicet.gov.ar](mailto:dfalaschi@mendoza-conicet.gov.ar)

observed. In comparison with other clusters worldwide, surge-type glaciers in the Central Andes are on average smaller and show minor absolute advances. Generally low velocities and the heterogeneous duration of the surge cycles are common between them and glaciers in the Karakorum, a region with similar climatic characteristics and many known surge-type glaciers. As a definitive assertion concerning the underlying surge mechanism of surges in the Central Andes could not be drawn based on the remote sensing data, this opens more detailed research avenues for surge-type glaciers in the region.

### Keywords

Surge-type glacier, glacier elevation change, glacier surface velocity, glacier mass balance, Central Andes

## 1 Introduction and previous studies

Although surge-type glaciers represent a minor portion of the world's total number of glaciers, they have been documented in several mountain ranges of the world, such as Alaska, Arctic Canada, Greenland, Svalbard, the Karakorum and Pamir, and are most frequently grouped in clusters (Sevestre and Benn, 2015). Despite a relatively large number of them having been studied, there is at present arguably insufficient quantitative information to accurately define what a glacier surge is (Harrison and Post, 2003; Mukherjee et al., 2017; Raymond, 1987). Nor has a given advance rate over a specific time period been firmly established for a given glacier to fall in the surge-type glacier category. Currently, however, there is general consensus on three main criteria for the identification of a surge-type glacier: (1) quasiperiodic cycles in ice flow velocities characterized by *surging* or *active* phases of 1–15 years duration (Jiskoot, 2011), when velocities can be at least 10–1000 times higher than the balance velocity (Benn and Evans, 2010; Dowdeswell et al., 1991), and *passive* or *quiescent* phases (tens to hundreds of years), when velocities are less than the balance velocity (Jiskoot, 2011); (2) ice terminus advance, which is out of synchrony with the behavior of neighboring glaciers (Sevestre and Benn, 2015); and (3) the presence of morphological features such as looped moraines indicating a tributary surge, heavily (often chaotically) crevassing on the glacier surface,

surface potholes and sheared margins, among others (Barrand and Murray, 2006; Copland et al., 2003; Grant et al., 2009).

Prior to the onset of the glacier surge and during the *buildup* phase, a steepening of the glacier surface occurs as a result of a restricted outflow and the ice mass increases in the reservoir area until the active phase is initiated. Throughout this phase, ice is transferred from the reservoir area to the receiving area in the lowermost part of the glacier, often leading to an exceptional advance of the glacier front (Meier and Post, 1969). As a result of the ice transfer process, ice removal from the reservoir area causes lowering of the glacier surface, whereas the receiving area thickens (Benn and Evans, 2010). Following surge termination, the glacier surface flattens and crevasses close (Pitte et al., 2016), and relative low elevation of the glacier terminus leads to a temporarily accelerated ablation rate and frontal retreat (Yde and Knudsen, 2007). Also, portions of the lowermost part of a surging glacier can detach and be left as stranded, dead ice (Weidick, 1988), which can be interpreted as a sign of past dynamics.

The development of a surge in relation to velocities throughout the full event has led to propose two different surge models (Jiskoot, 2011). Two-phase cycle surges are characterized by an abrupt change between glacier velocities in the quiescent and active phases, a sustained fast flow throughout the surge and rapid surge termination, whilst three-phase

surges have a long quiescent phase, a prolonged (months to years) period after which the glacier velocity reaches a maximum, and a final stage of slowly diminishing velocities. Each of these two surge models have been linked to a correspondent hypothesis relative to a thermal (Alaska-type) or hydrological (Svalbard-type) surge control. Moreover, these two mechanisms imply observable differences regarding the time of the year at which surges initiate and terminate. In Alaskan-type (temperate glaciers), surge initiation occurs mainly in winter and termination in summer, whereas in Svalbard-type (polythermal glaciers), a surge can begin and end at any time of the year (Jiskoot, 2011 and references therein).

Identification and monitoring of glacier surges is of particular relevance, since they may pose major hazards. The sudden advance of a surging glacier may lead to river damming (Bruce et al., 1987; Harrison et al., 2015; King, 1934). The newly-formed ice dam may in turn collapse and release a glacial lake outburst flood (Round et al., 2017). Other hazards relate to catastrophic water discharges from the subglacial drainage system following surge termination and terrain movements caused by river damming. Such hazards can greatly affect human settlements and infrastructure (Kääb et al., 2005a).

In the Central Andes, much attention has been given to the Grande del Nevado del Plomo glacier (Plomo hereafter) owed to its major hazards. An outburst flood was released from the dammed lake following the breakup of the ice dam which formed after the surge that culminated in 1934, when the glacier advanced 900 m (Espizua, 1986) at an estimated rate of  $25 \text{ m d}^{-1}$ . In early 1935, a flood flowed downstream of the glacier for dozens of kilometers along the Plomo and Mendoza river valleys, destroying several infrastructure facilities, including the Cacheuta hydropower station (King, 1934, 1935). Apprehension was raised again in 1984, when the Plomo glacier surged again advancing 2.5 km at an average  $16 \text{ m d}^{-1}$

rate between February–November (Pitte et al., 2016). This time around, however, the dammed lake drained gradually via a subglacial conduit (Bruce et al., 1987; Espizua and Bengochea, 1990). No ice dam formed in the 2007 Plomo surge. During this latter surge, the glacier advanced 3 km at a  $35 \text{ m d}^{-1}$  velocity (Leiva, 2006; Pitte et al., 2016).

Also, the Horcones Inferior glacier (hereafter Horcones) in the Mt. Aconcagua massif, surged at least twice during the last four decades. Previously, Cox et al. (1935), had mentioned that the Horcones might cause similar inconveniences to the Plomo glacier, since the glacier had advanced a half mile between 1895–1924. A sketch by Sievers (1903) depicts in fact the Horcones glacier snout in a position resembling that of later surges. In a surge episode that took place between 1984–1990 (Unger et al., 2000), Horcones sped up from less than  $0.1 \text{ m d}^{-1}$  to nearly  $9 \text{ m d}^{-1}$  (Lenzano et al., 2011), whereas during the 2002–2005 surge, velocities increased up to  $14 \text{ m d}^{-1}$  (Pitte et al., 2016). During this surge, the advance of Horcones forced the relocation of Confluencia, a semi-permanent intermediate camp en route to Mt. Aconcagua (Pitte et al., 2016).

Beyond the aforementioned well-known Horcones and Plomo surges, a number of authors have indicated other glaciers in the Central Andes as surge-type (Table 1). These studies, however, are generally descriptive in nature and contain little, if any information on surge timing, length, area, volume and velocity changes. In the early twentieth century, Helbling (1935) conducted an exploration trip in the Plomo catchment and came to the conclusion that Grande del Juncal glacier had an analogous behavior to that of Plomo, but did not quantify any glacier change. Cobos and Boninsegna (1983) used aerial photographs to detect the 1.4 km advance of Laguna glacier between 1970 and 1982, and suggested the possibility of a glacier surge. Llorens and Leiva (1995), using Landsat imagery, reported a 2.9 km advance of Innominado glacier in the Plomo catchment

**Table 1.** Summary of current knowledge about surge-type glaciers in the Andes, as currently included in the WGMS database. In the RGI ID column, codes in brackets are previously incorrectly identified glaciers.

Name of glacier/ location	RGI ID	Surge periods	Reference	Evidence of surges	Calculations		Surge Index
					length	velocity	
Horcones/ 32.67 S 70.00 W	60-17 14140	1895–1924 1984–1990 2002–2007	Cox et al., 1935; Sievers, 1903 Happoldt and Schrott, 1993; Unger et al., 2000 Milana, 2004; Lenzano et al., 2011, 2013; Pitte et al., 2016	historical accounts geomorphologic, field investigations, satellite data geomorphologic, field investigations, satellite data historical accounts	✓ ✓ ✓	✓ ✓ ✓	I
Plomo/ 33.07 S 70.03 W	60-17 13949	1786 1912–1934	Prieto, 1986 King, 1934, 1935; Helbling, 1935; Espizúa, 1986	geomorphologic, field investigations, aerial photographs aerial photographs field investigations, satellite data	✓	✓	I
Noreste del Cerro Alto/ 33.27 S 69.85 W	60-17 13798	1962–1974 1984 2004–2007 1946	Casassa et al., 1998 Bruce et al., 1987; Espizúa, 1987; Espizúa and Bengochea, 1990 Pitte et al., 2016 Liboutry, 1999	satellite data geomorphologic, historical accounts geomorphologic geomorphologic, historical accounts	✓ ✓	✓ ✓	I
Piuquenes/ 33.29 S 69.48 W	60-17 13798	1986 1997	Liboutry, 1999 Liboutry, 1999	geomorphologic geomorphologic, historical accounts			I
Cachapoal/ 34.31 S 70.03 W	60-17 13403	1848	Plagemann, 1887; Rothlisberger, 1986	historical accounts			I
Grande del Juncal/ 33.05 S 70.08 W	60-17 14027	1910	Helbling, 1935	geomorphologic, field investigations, satellite data, aerial photographs	✓	✓	I
Colina/ 33.97 S 69.84 W	60-17 13608 (60-17 13624)	1934–1955 1937	Espizúa, 1986, 1987 Liboutry, 1999	geomorphologic geomorphologic	✓	✓	I

(continued)

**Table 1.** (continued)

Name of glacier/ location	RGI ID	Surge periods	Reference	Evidence of surges	Calculations	
					length	Surge Index velocity
Marmolejo/ 33.73 S	60-17 - 17 13081	19??	Lliboutry, 1999	geomorphologic		2
69.85 W						
Nieves Negras/ 33.49 S	60-17 13633	1927	Lliboutry, 1956, 1999	geomorphologic		1
69.54 W						
Polleras/ 33.15 S	60-17 13839	19??	Lliboutry, 1999	satellite data		2
69.54 W						
Innominado/ 33.09 S	60-17 13907	1986–1991	Llorens and Leiva, 1995	satellite data	✓	1
70.03 W						
Río Museo/ 33.30 S	19809 (60-17 13841)	1935	Lliboutry, 1956, 1999	geomorphologic		1
69.52 W						
Universidad/ 34.39 S	60-17 01986	1943	Lliboutry, 1958	geomorphologic		1
70.21 W						
Juncal Sur/ 33.04 S	60-17 14015	1947	Lliboutry, 1956; Masiokas et al., 2009	historical accounts	✓	1
70.05 W						
Laguna/ 34.29 S	60-17 01218	1970–1982	Cobos and Boninsegna, 1983	aerial photographs	✓	1
70.06 W						

between 1986 and 1991. Lliboutry (1999) suggested surge-type behavior for Río Museo, Marmolejo, Colina, Polleras, Piuquenes, and Noreste del Cerro Alto glaciers based on geomorphologic interpretations of remote sensed data, but provided no direct/indirect measurements whatsoever.

Further surges have been identified based on historical documents and accounts, as in the cases of Cachapoal (Plagemann, 1887; Rothlisberger, 1986), Nieves Negras (Lliboutry, 1956), and Plomo (Prieto, 1986). The advance of Juncal Sur in 1947 (Lliboutry, 1956) culminated in the formation of a small lake and interrupted the operation of El Alfalfal hydropower station. Also in the Central Andes, Lliboutry (1958) mentioned the surging behavior of Universidad glacier in 1943, though no further surge evidences were identified since then (Wilson et al., 2016).

Many of the aforementioned glaciers lie in the headwaters of mountain rivers that supply fresh water to not too distant areas of agriculture and human settlements. With the precedent of the hazards posed by some of them, it is particularly surprising that so little is known about their surge-type behavior. Monitoring of glacier surges is hence of particular importance (Kääb et al., 2005b), and with the increasing volume of satellite imagery and digital elevation models (DEMs) available, more surge-type glaciers and clusters are recognized (e.g. Grant et al., 2009; Mukherjee et al., 2017).

The aim of this study is therefore (1) to revisit the glaciers for which fragmentary data and descriptions suggesting surge-type behavior has been previously reported but not exhaustively explored, providing complementary information regarding absolute and relative glacier advances, elevation changes and improved timing of the surge events; (2) present additional, detailed information about the relatively well investigated Horcones and Plomo glaciers; and (3) search for new evidence of glaciers showing surge-type characteristics with the ultimate goal

to generate an up-to-date inventory of surge-type glaciers for the Central Andes of Argentina and Chile, including the period and characteristics of the surges, glacier-specific morphological information (slope, aspect, minimum elevation, length, area) and a surge-type glacier indexation. Given the fairly coincident timing of the last two surge events for both the Horcones and Plomo glacier surges, we had a close examination of glacier behavior (e.g., changes in surface elevation and velocity) in the region during the 2000–2011 timespan, which covers the active phases of the latest Horcones and Plomo surges.

## II Study area

The study area is encompassed in the Central Andes of Argentina (Mendoza Province) and Chile (V–VI regions) amid 32° 40'–34° 20' S (Figure 1). The region is characterized by high relief, including some of the highest peaks of the entire Andes such as Volcán Tupungato (6570 m) and Mt. Aconcagua (6962 m). The Central Andes (31–35° S) represent a relatively densely glacierized region in comparison with the immediately bounding regions. North of 31° S, in the so-called Arid Andes, the scarce precipitation is barely sufficient for the generation of large glaciers. Even above altitudes of 6000 m a.s.l., ice mostly appears in the form of small-sized glaciers “glacier reservoir” (Lliboutry, 1956) atop high volcanoes. Further south, between 35–45° S, the comparatively lower Northern Patagonian Andes host a significantly minor number of glaciers, associated with large but isolated volcanic edifices (Rivera et al., 2012; Rivera and Bown, 2013).

The climate in the high Central Andes is characterized by a Mediterranean regime, with snowfall precipitation maxima during the austral winter (June–August) brought by frontal systems driven in turn by the westerly flow (Garreaud, 2009). Masiokas et al. (2012) compiled data from tree ring and rainfall records to

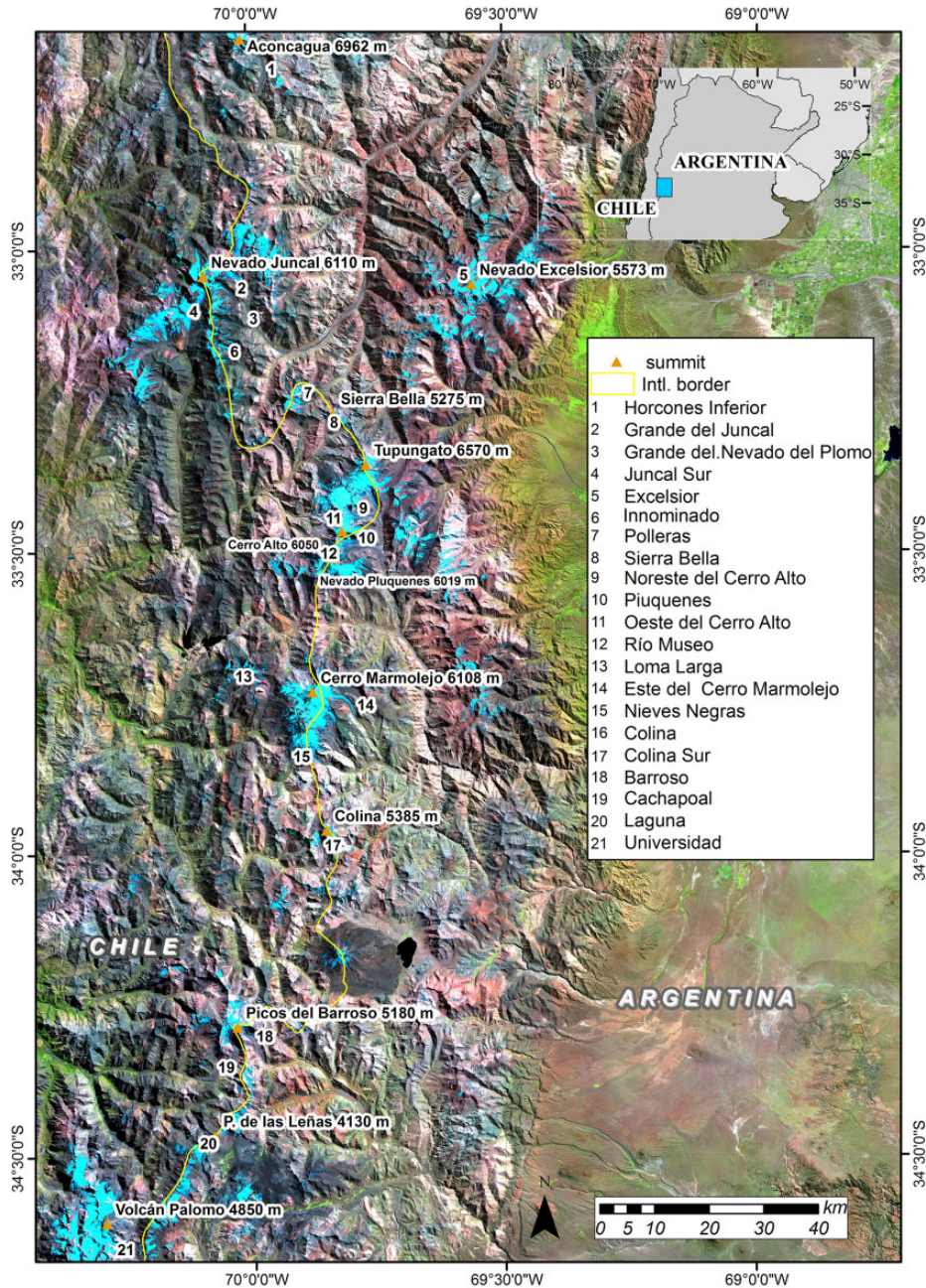


**Figure 1.** Location of the study area (in light blue in the inset) and all the glaciers mentioned in the text.

find a negative precipitation trend over the last 100–150 years in the Central Andes. Using winter maximum snow water equivalent data from eight high elevation meteorological, Falaschi

et al. (2016) found no significant trend in snow precipitation, but rather a random succession of humid and dry periods stations for the 1951–2013 period. Conditions were particularly dry

during the 1990s and from the year 2005 onwards. In relation to temperature records, the ERA interim reanalysis showed a relatively warm interval during the 1980's, followed by a temperature drop in the 1990s and a moderate increase in temperatures since the beginning of the 2000s (Masiokas et al., 2016).

Glaciers between 31° and 38° S are subjected to mean annual precipitation exceeding 950 mm above 2000 m a.s.l. (Masiokas et al., 2012) and monthly temperatures ranging from  $-5.3^{\circ}\text{C}$  in the winter to  $5.5^{\circ}\text{C}$  in the summer (Sagredo and Lowell, 2012). The snowline in this region decreases from 5000 m to  $\sim 2800$  m a.s.l. from north to south (Condom et al., 2007; Nogami, 1972). In addition to the relatively scarce and highly variable precipitation, the great thermal amplitude, strong winds and high incoming solar radiation result in enhanced rock weathering rates, which result in extensive (up to one third of the glacier area; Bown et al., 2008) debris covers on glacier snout. Glaciers vary from predominantly polythermal to cold-based with slow flow rates in the north to temperate and faster flowing glaciers in the south (Milana, 2010).

### III Data

#### *I Landsat and corona satellite imagery, aerial photographs, and topographic maps*

We used orthorectified (processing level L1 T) Landsat MSS, TM, and ETM+ images (ETM+ is affected in this area by the failure of the Scan Line Corrector in the year 2003, hence the small number of ETM+ scenes) from the years 1976 to 2011 to map and delineate the outlines of the investigated surge-type glaciers (Appendix A). Also for glacier mapping purposes, we used high resolution imagery available from Google Earth (typically Geoeye, WorldView for this region) spanning from 2003 to 2015, declassified 1967 Corona KH4-A scenes, and 1962 and 1974 aerial photographs from IANIGLA's and the Servicio Geológico Minero of Argentina

(SEGEMAR) archives. Not all the satellite and especially the aerial imagery data were available for all of the investigated glaciers. The oldest glacier data corresponds to the Grande del Juncal glacier outline as measured during several field campaigns conducted between 1909 and 1912, and is provided by a topographic map elaborated during the topographic surveys of Dr. Robert Helbling in the Central Andes (Helbling, 1919; Schellenberger, 2014).

Additional Landsat TM imagery was used to retrieve glacier surface velocities during the active phases of the Piuquenes and Noreste del Cerro Alto surges in the mid-1980s and mid-2000s. The investigated glaciers are located in areas of data gaps in the higher spatial resolution Landsat ETM+ satellite images after the failure of the scan line correction, which hampers glacier delineation and velocity determinations. All Landsat TM and Corona imagery was downloaded from the USGS through the Earth Explorer data poll at <http://www.earthexplorer.usgs.gov>.

#### *2 DEMs: shuttle radar topography mission synthetic aperture radar (SRTM) and ALOS panchromatic remote-sensing instruments for stereo mapping (PRISM)*

Using interferometric synthetic aperture radar (SAR) sensors in C-band, the Shuttle Radar Topography Mission acquired data between February 11 and February 22, 2000. A nearly global ( $60^{\circ}\text{N}$ – $56^{\circ}\text{S}$ ; Farr et al., 2007) DEM was produced at 1 arcsec resolution for the SIR-C sensor. Here we used void-filled SRTM grids, also downloaded from the Earth Explorer portal. Tiles were sampled to 30 m resolution and projected in the UTM Zone 19 South projection.

Rignot et al. (2001) have pointed out the SRTM C-band underestimation of glacier elevation in comparison with the X-band, owed to the deeper penetration of the radar pulse into the snow cover at the comparatively longer 5.6 cm



wavelength (SRTM X band wavelength = 3.1 cm). Because all but one of the investigated glaciers are heavily debris-covered, we expected no radar penetration in the ablation zone of these glaciers. Furthermore, SRTM was acquired during the ablation period in the Andes of Argentina and Chile, when the glacier surface should have been reasonably devoid of fresh snow, precluding the penetration of the radar wave. Dehecq et al. (2016) have stated that the lesser penetration of the X-band is limited at high elevations, and the related error is acceptable for geodetic mass balance determinations for over 10 year assessments. Hence, no procedure was carried out to correct the elevation values of the SRTM C-band tiles.

Specifically for this study, we generated three sets of ALOS PRISM DEMs with a spatial resolution of 30 m (matching the SRTM DEM pixel size) with the Ortho-image Generation Software specially designed for PRISM data by the Japan Aerospace Exploration Agency. Extensive validation of PRISM DEMs using this procedure acknowledges a horizontal accuracy of less than 6 m and an absolute vertical error of 2–18 m (Takaku and Tadono, 2009). The DEM were extracted from 10 ALOS PRISM stereopairs (2.5 m resolution), dating from March 31 and April 17, 2011, and for Plomo glacier only, March 22, 2008 (Appendix A). Owing to low optical contrast in the highly reflective snow of the accumulation areas of some glaciers, the PRISM DEM presents 22.5% data voids over the glacier area mapped in this study. As with the SRTM DEM, the original PRISM scenes were acquired in an advanced stage of the dry season in the Southern Andes, and should therefore be largely devoid of seasonal snow on the glacier surface.

## IV Methods

### *I Identification of surge-type glaciers*

We identified surge-type glaciers on the basis of the satellite images and DEM difference grid

interpretation in addition to the potential surge-type glaciers identified from previous research (Table 1). From the three main characteristics of surge-type glaciers stated in the introductory section (i.e., changes from abnormal to surge velocities and back, terminus advance and indicative morphological features), the assessment of glacier velocity changes were limited to three surges (see Section IV.5), whilst glacier length changes were measured in all but three glaciers (Section IV.3). A precise determination of the duration of surge cycles is often severely hampered by the limited availability of archival imagery from the first half of the twentieth century and earlier on. Geomorphological evidence for glacier surges stems from a series of characteristics including large displacement of ice mass/volume gain to the lower ablation area, heavily crevassed surface, contorted or looped medial moraines, high speed flow and push moraines (Copland et al., 2003; Grant et al., 2009). The presence of these indicative features and the fulfillment of the two other criteria, coupled with other characteristics such as the direct/indirect observation of glacier surges has resulted in a number of surge-type indexations (e.g. Barrand and Murray, 2006; Copland et al., 2003, 2011; Sevestre and Benn, 2015; Yde and Knudsen, 2007). Here we use the latest surge-type index by Mukherjee et al. (2017), which adjusts the index by Sevestre and Benn (2015) and categorizes confirmed surge-type glaciers (index = 1), very probable surge-type glaciers (index = 2), and possible surge-type glaciers (index = 3). According to this classification, and in addition to the geomorphological features common to all three index, the average advance rate differs between confirmed surge-type ( $>100 \text{ m yr}^{-1}$ ), probable surge-type ( $100 \text{ m yr}^{-1} > \text{advance rate} > 10 \text{ m yr}^{-1}$ ), and possible surge-type ( $<10 \text{ m yr}^{-1}$ ).

Glacier denomination is crucial in this region, since the misleading of glacier names has resulted in erroneous location and count of

surge-type glaciers in the Andes in the present databases of the World Glacier Monitoring Service GMS (WGMS, 2017) and the current version of the Randolph Glacier Inventory (RGI 6.0, RGI Consortium 2017; Pfeffer et al. 2014) (see Table 2), which are based on Sevestre and Benn (2015). Currently, not many glaciers have official names in the study region. When available, we used glacier names from official Chilean ([www.dga.cl](http://www.dga.cl)) and Argentinean ([www.glaciaresargentinos.gob.ar](http://www.glaciaresargentinos.gob.ar)) cartography. Otherwise, the utilized denomination followed Lliboutry (1999) or alternatively, we named the glaciers according to the main peak from which the given glacier flows (e.g., Barroso glacier after Picos del Barroso). Noreste del Cerro Alto and Piuquenes glaciers are two of the three main tributaries of a mayor trunk glacier, which we termed Tunuyan (Figure 2). For the sake of clarity, RGI ID numbers are provided in Table 2.

A t-test was carried out to compare the topographic characteristics (area, length, slope, aspect, and minimum and maximum elevation) of the surge-type glaciers, as derived from the SRTM data, with respect to the non-surge-type ones. Topographic parameters of the non-surge-type glaciers in the Tupungato, Diamante, and Tunuyan catchments (851 glaciers in total) were culled from the Argentinean National Glacier Inventory (Inventario Nacional de Glaciares, ING) ([www.glaciaresargentinos.gob.ar](http://www.glaciaresargentinos.gob.ar)). This glacier inventory initiative contains much improved outlines in comparison to the Randolph Glacier Inventory. No non-surge-type glaciers in Chilean territory were used in the analyses.

## 2 Glacier ice mapping

Outlines for the investigated glaciers exist from the ING. These outlines are often based on very high resolution satellite imagery and are backed up by extensive terrain verification. Yet, the glacier polygons are exceedingly smoothed

(which makes them hardly adjustable to the original optical and DEM raster data), and correspond to recent years (>2009). Thus, the customary TM3/TM5 band ratio method and a  $DN > 2$  threshold for the delineation of bare ice in the Landsat scenes were used (see Bolch et al., 2010; Paul et al., 2002). The extent of the debris-covered ice was obtained from the glacier outlines produced by the ING, which were nonetheless manually adjusted to the glacier extent in the Landsat scenes of different years. Area changes were calculated between 2000 and 2011 in order to relate them to the corresponding contemporaneous elevation changes, no matter a given surge event started or lasted beyond the 2000–2011 study period.

Uncertainties in glacier elevation changes and mass budget determinations by means of DEM differencing (i.e., the geodetic method) strongly depend on the mean glacier size (Zemp et al., 2013). Thus, highly accurate glacier outlines are required. The corresponding 2000 and 2011 glacier outlines were checked for seasonal snow against Landsat TM scenes from the years 1999 and 2010. For the purpose of this study, we assumed that the mapping uncertainty in debris-covered ice on Landsat images equals half the TM pixel size (15 m) (Bolch et al., 2010; Paul et al., 2013). Based on this assumption, we expected a glacier area uncertainty of  $\sim 5\%$ , which is in line or slightly more conservative than previous studies.

## 3 Length changes

We calculated glacier length changes along a central flow line using the satellite images by visual interpretation. The flow line was drawn perpendicular to the contour lines derived from the SRTM and upwards from the glacier snout. The line was then cropped using the glacier outlines produced for each measurement year. Because all imagery is projected in UTM Zone 19 S, length measurements are provided as projected distances. In the cases of Barroso, Colina

**Table 2.** Main characteristics of identified surge-type glaciers in the Central Andes. In the RGI ID column, codes in brackets are previously incorrectly identified glaciers. Mass balance values in brackets refer to the active glacier tongues \* not calculated.

Glacier	RGI ID	Advance period	Length (km)	Advance rate (m yr <sup>-1</sup> )	Relative length change (%)	Advance (m)	Mean slope (°)	Minimum elevation (m)		dh/dt (m yr <sup>-1</sup> )	Mass balance (m w.e. yr <sup>-1</sup> )
								Area (km <sup>2</sup> )	Area (km <sup>2</sup> )		
Barroso	17 13402	1986–2015	L <sub>1986</sub> = 4428	10	6.8	303 ± 30	19.7	Me <sub>2000</sub> = 2963	A <sub>2000</sub> = 8.1	–	0.26 ± 0.31
			L <sub>2015</sub> = 4731					Me <sub>2011</sub> = 2963	A <sub>2011</sub> = 8.1	–	(0.59 ± 0.31)
Colina	17 13608 (17 13624)	1967–1976	L <sub>1967</sub> = 2888	114	35.5	1026 ± 60	18.8	Me <sub>2000</sub> = 3619	A <sub>2000</sub> = 2.4	–	–0.37 ± 0.24
			L <sub>1976</sub> = 3914					Me <sub>2011</sub> = 3464	A <sub>2011</sub> = 2.5		
			L <sub>1967</sub> = 4252								
Colina Sur	17 13609	1986–2015	L <sub>2013</sub> = 4425	38	4.1	338 ± 30					
			L <sub>1986</sub> = 6019	19	16	960 ± 30	15.2	Me <sub>2000</sub> = 3297	A <sub>2000</sub> = 7.7	–	–0.02 ± 0.25
			L <sub>2013</sub> = 6979					Me <sub>2011</sub> = 3297	A <sub>2011</sub> = 7.7		(0.1 ± 0.25)
Cachapoal	17 13403	–	L <sub>1986</sub> = 7766	–	–	–	20	Me <sub>2000</sub> = 2523	A <sub>2000</sub> = 15.0	1.01 ± 0.31	–
			L <sub>2013</sub> = 8748					Me <sub>2011</sub> = 2523	A <sub>2011</sub> = 15.0	(1.45 ± 0.31)	
			L <sub>1986</sub> = 6241	16	2.8	176 ± 30	25.1	Me <sub>2000</sub> = 3245	A <sub>2000</sub> = 9.7	–	–0.09 ± 0.31
Loma Larga	17 13710	2004–2015	L <sub>2000</sub> = 6241					Me <sub>2011</sub> = 3245	A <sub>2011</sub> = 9.7	–	(0.02 ± 0.31)
			L <sub>2011</sub> = 6417	42	–1.2	–	21.8	Me <sub>2000</sub> = 3386	A <sub>2000</sub> = 14.7	~0 ± 0.32	–
			L <sub>2000</sub> = 10,128	71	9.8	997 ± 60	–	Me <sub>2011</sub> = 3378	A <sub>2011</sub> = 14.5	–	–
Marmolejo	17 - 17 13081	2004–2007	L <sub>1976</sub> = 11,127								
			L <sub>2000</sub> = 10,130	1030	37.4	3090 ± 42	18.7	Me <sub>2000</sub> = 3742	A <sub>2000</sub> = 8.2	–	–0.48 ± 0.38
			L <sub>2011</sub> = 11,345					Me <sub>2011</sub> = 3521	A <sub>2011</sub> = 10.1		
Horcones	17 14140	2002–2005	L <sub>2000</sub> = 8255	32	2.8	224 ± 42	44.8	Me <sub>2000</sub> = 3633	A <sub>2000</sub> = 10.2	0.24 ± 0.32	–
			L <sub>2011</sub> = 8073					Me <sub>2011</sub> = 3581	A <sub>2011</sub> = 10.3		
			L <sub>1962</sub> = 10130	74	11	858 ± 60	–				
Grande del Juncal	17 14027	2006–2011	L <sub>2011</sub> = 8297								
			L <sub>1962</sub> = 7764	18	2.3	90 ± 30	30.4	Me <sub>2000</sub> = 4099	A <sub>2000</sub> = 3.1	–	–0.16 ± 0.29
			L <sub>1974</sub> = 8622					Me <sub>2011</sub> = 4004	A <sub>2011</sub> = 3.2		
Oeste del Cerro Alto	17 13760	2007–2012	L <sub>2000</sub> = 3890	23	25.4	784 ± 30	25	Me <sub>2000</sub> = 3774	A <sub>2000</sub> = 2.3	–	0.3 ± 0.29
			L <sub>2011</sub> = 3980					Me <sub>2011</sub> = 3654	A <sub>2011</sub> = 2.4		
			L <sub>2000</sub> = 3284					Me <sub>2000</sub> = 3414	A <sub>2000</sub> = 61.6	–0.3 ± 0.33	–
Sierra Bella	17 13824	1998–2012	L <sub>2011</sub> = 3864					Me <sub>2011</sub> = 3414	A <sub>2011</sub> = 61.6	–	–
			L <sub>2000</sub> = 20094					Me <sub>2000</sub> = 4434	A <sub>2000</sub> = 5.9	–0.05 ± 0.30	–
			L <sub>2011</sub> = 20094					Me <sub>2011</sub> = 4401	A <sub>2011</sub> = 6.0		
Tunuyan	17 13798	2003–2007	L <sub>2000</sub> = 20094					Me <sub>2000</sub> = 2426	A <sub>2000</sub> = 30.3	–0.56 ± 0.30	–
			L <sub>2011</sub> = 20094					Me <sub>2011</sub> = 2433	A <sub>2011</sub> = 30.4		
			L <sub>2000</sub> = 5511					Me <sub>2000</sub> = 3776	A <sub>2000</sub> = 21.9	–1.08 ± 0.27	–
Excelisior	17 20152	2000–2007	L <sub>2011</sub> = 5511					Me <sub>2011</sub> = 3806	A <sub>2011</sub> = 21.7		
			L <sub>2000</sub> = 10,302								
			L <sub>2011</sub> = 10,414								
Universidad	17 01218	–	L <sub>2000</sub> = 10,071								
			L <sub>2011</sub> = 10,071								
			L <sub>2011</sub> = 10,138								
Juncal Sur	17 14015	–	L <sub>2011</sub> = 10,138								

(continued)

Table 2. (continued)

Glacier	RGI ID	Advance period	Length (km)	Advance rate (m yr <sup>-1</sup> )	Relative length change (%)	Advance (m)	Mean slope (°)	Minimum elevation (m)		Area (km <sup>2</sup> )	dh/dt (m yr <sup>-1</sup> )	Mass balance (m w.e. yr <sup>-1</sup> )
								Me <sub>2000</sub>	Me <sub>2011</sub>			
Nieves Negras	17 013633	-	L <sub>2000</sub> = 7358	-			23.2	Me <sub>2000</sub> = 3139	A <sub>2000</sub> = 8.2	-	-0.15 ± 0.3	-
			L <sub>2011</sub> = 7358					Me <sub>2011</sub> = 3139	A <sub>2011</sub> = 8.2			
Laguna	17 01240	-	L <sub>2000</sub> = 4469	-			13.8	Me <sub>2000</sub> = 3247	A <sub>2000</sub> = 6.5	-	-	0.15 ± 0.26
			L <sub>2011</sub> = 4854					Me <sub>2011</sub> = 3288	A <sub>2011</sub> = 5.8			
Innominado	17 13907	-	L <sub>2000</sub> = 6163	-			15.7	Me <sub>2000</sub> = 3617	A <sub>2000</sub> = 3.9	-	-	-
			L <sub>2011</sub> = 6163					Me <sub>2011</sub> = 3617	A <sub>2011</sub> = 3.9			
Plomo	17 13949	-	L <sub>2000</sub> = 4613	-			19.7	Me <sub>2000</sub> = 3669	A <sub>2000</sub> = 2.2	-	-0.06 ± 0.27	-
			L <sub>2011</sub> = 8280					Me <sub>2011</sub> = 3192	A <sub>2011</sub> = 4.4			
Rio Museo	17 13837	-	L <sub>2000</sub> = 3002	-			35.1	Me <sub>2000</sub> = 4111	A <sub>2000</sub> = 1.6	-	-	0.19 ± 0.35
			L <sub>2011</sub> = 2867					Me <sub>2011</sub> = 4221	A <sub>2011</sub> = 1.5			
Polleras	17 13839	-	L <sub>2000</sub> = 3842	-			20.8	Me <sub>2000</sub> = 3756	A <sub>2000</sub> = 4.2	-	-	0.1 ± 0.31
			L <sub>2011</sub> = 4123					Me <sub>2011</sub> = 3844	A <sub>2011</sub> = 4.1			

2000–2011

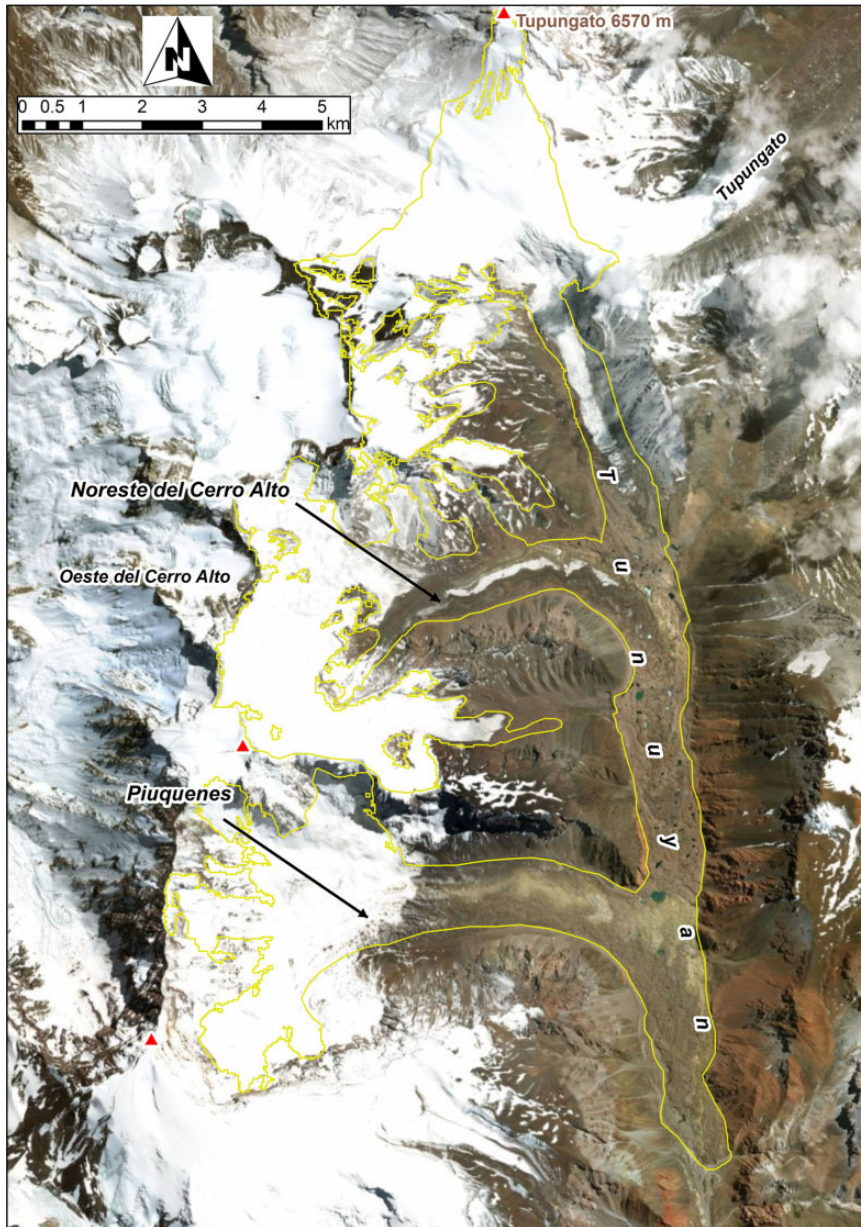


**Figure 2.** Detail of the Tunuyan trunk glacier and the Noreste del Cerro Alto and Piuquenes tributaries, with the glacier outline in yellow line. Image source: Google Earth©.

Sur, Loma Larga, Cachapoal, and Este del Cerro Marmolejo (Marmolejo hereafter) glaciers, inactive, debris-covered tongues (dead ice) lies ahead of the active surge fronts. For the length calculations, only the active tongue was considered. In

the cases of the Tunuyan tributaries (Noreste del Cerro Alto and Piuquenes), and due to the difficulties in determining the limit between the tributary and trunk glaciers, we did not calculate the length changes of the tributaries.

The uncertainty in glacier length estimations  $\epsilon\Delta L$  (m) between each pair of scenes was calculated after Hall et al. (2003), considering the different satellite imagery pixel size in meters ( $ps$ ) and the co-registration error  $CE$  (m) between successive scenes as

$$\epsilon\Delta L = \sqrt{ps_1^2 + ps_2^2} + CE \quad (1)$$

Because L1 T Landsat scenes are properly orthorectified, their horizontal coordinates have a good match and no co-registration is needed. This way, the term  $CE$  in equation (1) can be discarded when using L1 T data only.

#### 4 Co-registration of DEMs and mass balance calculation

We used the method developed by Berthier et al. (2007) to remove the horizontal and vertical shifts between the SRTM and PRISM DEM. This procedure shifts iteratively a slave DEM (PRISM in our case) with respect to a master DEM (SRTM) until a minimum in the standard deviation of the elevation differences over stable terrain is reached. Contrary to the PRISM DEM, whose elevation data refers to the WGS84 ellipsoid, the elevation values in the SRTM products correspond to the EGM96 geoid. Hence, ahead of DEM differencing, all elevation data is stacked in a single file, put in the same ellipsoidal datum and then projected in UTM Zone 19 South.

Once the DEMs were co-registered, we calculated glacier elevation changes ( $dh/dt$ ) between February 2000 ( $t_0$ ) and March-April 2011 ( $t_1$ ) by subtracting the newer PRISM to the older SRTM DEM. For the Loma Larga, Cachapoal, Tunuyan, Colina Sur, and Barroso glaciers, which have dead ice below the active glacier tongues, we calculated the glacier elevation changes considering both the active and inactive ice extent.

Large voids in the PRISM DEMs in the upper parts of some glaciers prevented a meaningful elevation change of the full glacier area. Several

ways to deal with data gaps exist, such as filling the data voids with the mean elevation change calculated on the basis of elevation bands (see Le Bris and Paul, 2015). Because in some glaciers our data gaps were considerably large, sometimes missing more than half the glacier area, we considered that the interpolation of missing values would seriously alter the  $dh/dt$  signal and thus retained the data voids in the resultant elevation difference grids. We hence present here the  $dh/dt$  elevation changes of the covered (mostly lowermost) portions of these glaciers only, which still gives valuable insight, whilst we provide geodetic mass balance estimations for those glaciers fully captured in the DEM difference grids. Only a very small fraction of Innominado glacier was covered by the ALOS PRISM DEMs; the glacier was thus discarded from the elevation change calculations.

We also calculated rough thickness changes in the reservoir and receiving areas of the Noreste del Cerro Alto, Piuquenes, Horcones, and Plomo glaciers. For this purpose, the reservoir area was defined as those pixels showing positive elevation difference values (mass gain), whilst the receiving area is composed of pixels with negative values (mass loss) (Pitte et al., 2016).

To convert the glacier elevation change values into geodetic mass balance, the  $dh/dt$  values and glacier areas are used to calculate the volume change ( $\text{km}^3$ ) for each glacier. In this manner, the geodetic mass balance (m w.e.) can be calculated by assuming an average firn density conversion factor of  $850 \pm 60 \text{ kg m}^{-3}$  (Huss, 2013).

**4.1. Uncertainties.** In this study, surface elevation and mass changes uncertainties are mainly given by the errors of the two DEMs used. When determining glacier elevation and mass changes by means of DEM differencing, the approach suggested by Gardelle et al. (2013) is widely used to estimate the uncertainty (e.g. Bolch et al., 2017; Falaschi et al., 2017; Maurer et al., 2016). Here we follow the aforementioned method, which accounts for the degree of the spatial correlation

of the elevation differences over stable (off-glacier) terrain (Fischer et al., 2015). Because the slope and roughness of stable terrain way off the glaciers might be not entirely representative of the glacier surface (Rolstad et al., 2009), the uncertainty in elevation change was calculated for buffer areas around each glacier unit, of about two times the glacier area (Fischer et al., 2015). Finally, outliers were defined as (i) elevation change pixel values exceeding  $\pm 100$  m and (ii) stable terrain slope pixels greater than the mean slope plus one standard deviation of the glacierized areas and eliminated from the buffer areas. After removal of the slope outliers,  $\sigma$  of the elevation differences between the SRTM and PRISM DEMs on stable terrain was 7.7 m.

Uncertainty values were calculated for elevation bands (50 m here) as proposed by Gardelle et al. (2013) within the buffer areas encompassing the 2600–7000 m elevation span of the glacierized area. The standard error  $E\Delta z_i$  of the elevation differences between DEMs over stable terrain per elevation band is obtained by dividing the random error of each individual pixel of elevation change  $\sigma\Delta z_i$  by the effective number of independent values on each elevation band  $n_{eff}$ :

$$E\Delta z_i = \frac{\sigma\Delta z_i}{\sqrt{n_{eff}}} \quad (2)$$

In turn,  $n_{eff}$  is smaller than  $n_{tot}$  by a factor of  $2d$ :

$$n_{eff} = \frac{n_{tot} \cdot R}{2d} \quad (3)$$

$d$  being the distance of spatial autocorrelation (120 m) as calculated using the Moran's I autocorrelation index (Gardelle et al., 2013), and  $R$  (30 m) the pixel size.

The systematic uncertainty in the volumetric change calculations  $\epsilon\Delta z_i$  is calculated following (Koblet et al., 2010):

$$\epsilon\Delta z_i = \frac{\sum_1^n \Delta z_i}{n_{tot}} \quad (4)$$

where  $\Delta z_i$  (in meters) is the mean elevation difference between the two used DEMs and  $n_{tot}$  the total number of pixels.

For each glacier, the associated uncertainty in volume change  $E\Delta v_i$  results from the product of the area of each one of the elevation bands  $A_i$  ( $m^2$ ) and the corresponding uncertainty in elevation change:

$$E\Delta v_i = \sum_i^n E\Delta z_i * A_i \quad (5)$$

The  $\pm 60$   $kg\ m^{-3}$  uncertainty (Huss, 2013) is incorporated in the overall volume uncertainty calculation, taking into account the differences between using a density of  $790$   $kg\ m^{-3}$  and  $910$   $kg\ m^{-3}$  versus the  $850$   $kg\ m^{-3}$  reference value. This way, the overall volume change uncertainty ( $E\Delta_{v,tot}$ ) is calculated based on the standard principles of error propagation, where the error in volume change  $E\Delta v_i$  ( $m^3$ ) and the error in firm density assumption in meters ( $E_\rho$ ) are summed quadratically:

$$E\Delta_{v,tot} = \sqrt{E^2\Delta v_i + E^2\rho} \quad (6)$$

## 5 Glacier surface velocities and related uncertainty

We estimated glacier surface velocities of the Piuquenes and Noreste del Cerro Alto tributary glaciers during the two latest 1985–1987 and 2003–2007 surges. The choice of these two glaciers resided in a number of reasons. On one hand, and apart from Horcones and Plomo glaciers, Piuquenes and Noreste del Cerro Alto showed the most distinctive morphological surge-like features and were the glaciers where the mass transfer from the reservoir to the receiving zone were most clearly defined in the elevation difference maps. On the other hand, Piuquenes and Noreste del Cerro Alto were the two only glaciers where the combination of the image resolution, size of the trackable features, glacier velocity and time span between available imagery allowed a technically sounding

estimation of glacier velocities. The remaining glaciers had too small morphological features to be tracked in the comparatively coarser Landsat imagery, or flowed too slowly in relation to the time span between available satellite images (see below).

We applied the CIAS feature-tracking procedure (Kääb and Vollmer, 2000) on a series of Landsat images to determine glacier displacements. The CIAS procedure has been widely used in glaciological studies (e.g. Kumari et al., 2014; Smith et al., 2015; Wilson et al., 2016) since it has proven to yield accurate results in glaciers with high optical contrast (Heid and Kääb, 2012). We examined surface velocities on these surge-type glaciers during the mid-2000s surges and also calculated surface velocities for a previous Noreste del Cerro Alto surge in the mid-1980s.

In a first step, the initial  $t_0$  (first epoch) and the final  $t_1$  (second epoch) scenes are co-registered at sub-pixel scale utilizing the normalized cross-correlation (NCC) algorithm that uses CIAS (Kääb and Vollmer, 2000). Such algorithm operates by iteratively shifting a pixel block or window in the  $t_0$  image that is correlated to a second, usually larger window in the overlapping area of the  $t_1$  scene. Displacement magnitude and direction are determined by comparing the coordinates of the highest correlation block in the search window, with those of the first pixel block. Keeping an initial pixel block of  $15 \times 15$ , the final window varied between  $6 \times 6$  to  $9 \times 9$  pixels depending on the dissimilar glacier velocities at different times during a surge. The raw displacement values were filtered discarding points with  $< 0.6$  correlation coefficient (see Wilson et al., 2016), whilst abnormally low/high values were manually removed. Lastly, the CIAS-derived output points were converted to raster format and velocity maps produced.

The uncertainty in surface velocity estimations using cross correlation techniques stems

from basically three sources: (1) the image co-registration process, (2) the quality of the scenes themselves, and (3) the performance of the cross-correlation algorithm. Normally, an accuracy of  $\pm 2$  pixels can be expected for the co-registration of two Landsat TM scenes (Berthier et al., 2003) and hence the systematic error is defined as

$$\sigma_{\text{sys}} = \frac{2R}{\Delta t} \quad (7)$$

where  $R$  is the pixel size (30 m) and  $\Delta t$  the time separation in days. The correlation algorithm determines the motion of the glacier features at the sub-pixel scale, the strength of the correlation and the inherent random error  $\sigma_{\text{rand}}$ , which is quantified over stable terrain, discarding glacier and shadow areas and steep terrain ( $> 25^\circ$ ) (Berthier et al., 2005). The total error in the glacier velocity assessment  $\sigma_{v_{\text{tot}}}$  is again calculated following the laws of error propagation:

$$\sigma_{v_{\text{tot}}} = \sqrt{\sigma_{\text{sys}}^2 + \sigma_{\text{rand}}^2} \quad (8)$$

## V Results

### *1 General characteristics of the identified surge -type glaciers*

We identified a total of 21 surge-type glaciers, two of which had well documented surges and thirteen others had surge events or surge-like features mentioned in earlier research. From the sum of fifteen previously reported surging glaciers, thirteen of them have been classified as index = 1 (confirmed surge); Polleras was the single index = 2 (probable surge) glacier, as Marmolejo glacier is here updated from possible to probable surge (Table 3). In addition to these known surge-type glaciers, six glaciers are here considered as possible (index = 3) surge-type for the first time. Also, we defined eleven new surge events of variable duration among the 21 surge-type glaciers (Table 2).



**Table 3.** Classification of surge type glaciers, showing the fulfillment of the three general and the specific criteria of Mukherjee et al. (2017). The glaciers in the lower part of the table retain the indexation as found in the literature.

Glacier	Repeated surges	Measured velocity change	Volume gain in lower ablation region	Geomorphological features	Advance rate			Index
					>100 m yr <sup>-1</sup>	10 m yr <sup>-1</sup>	100 > x > 10 m yr <sup>-1</sup>	
Barroso	-	-	✓	dead ice		✓		3
Colina	✓	-	✓	crevassed surface, sheared margins		✓		1
Colina Sur	-	-	✓	dead ice, potholes		✓		3
Loma Larga	-	-	✓	dead ice, potholes,		✓		3
Marmolejo	✓	-	✓	contorted medial moraines, chaotically crevassed ice		✓		2
Horcones	✓	✓	✓	crevassed surface, potholes, significant and sudden advance	✓			1
Grande del Juncal	✓	-	✓	crevassed surface, sheared margins		✓		1
Oeste del Cerro Alto	-	-	✓	crevassed surface, sheared margins		✓		3
Sierra Bella	-	-	✓	dead ice		✓		3
Noreste del Cerro Alto/Piuguayes	✓	✓	✓	crevassed surface, contorted medial moraines, sheared margins, potholes	-			1
Plomo	✓	✓	✓	crevassed surface, sheared margins. dead ice, potholes, glacial lake outburst flood	✓			1
Excelsior	-	-	✓	push moraines?	-			3
Glacier surge data in literature								
Cachapoal	✓	-	✓	striking volume gain in the ablation area, dead ice, potholes, glacial lake outburst flood	-			1
Universidad	-	-	✓	-	-			1
Juncal Sur	-	-	✓	glacial lake outburst flood	-			1
Nieves Negras	-	-	✓	-	-			1
Laguna	-	-	✓	✓	✓			1
Innominado	-	-	✓	-	✓			1
Rio Museo	-	-	✓	-	-			1
Polleras	-	-	✓	-	✓			2

The areas of these glaciers are relatively small (mean area  $11.1 \text{ km}^2$ ) and except for Excelsior glacier, whose tongue is fully debris-free, all of the identified surge-type glaciers are heavily debris-covered, have overly steep accumulation areas and more gentle-sloping snouts ( $15\text{--}30^\circ$  average slopes).

The aspect of the surge-type glaciers is almost always East to South, which coincides with the prevailing aspect of glaciers in the Central Andes (Malmros et al., 2016); aspect differences between surge-type vs. non surge-type were not significant ( $p = 0.46$ ). We found that surge-type glaciers flow from higher elevations and reach lower elevations and are significantly larger, longer and flatter ( $p < 10^{-2}$ ) in comparison with non-surge-type glaciers.

## 2 Glacier length changes and advance rates

We found different responses in terms of relative length changes (Table 2). The most prominent advances were found for Plomo glacier. We roughly estimated  $3.3 \text{ km} \pm 0.06 \text{ km}$  ( $\sim 64\%$ ) and  $3.7 \text{ km} \pm 0.06 \text{ km}$  ( $\sim 80\%$ ) advances for the 1984 and 2004–2007 surges based on the surge front positions mapped in Pitte et al. (2016). During the minor 1962–1974 Plomo surge, the glacier terminus still advanced  $1.2 \text{ km} \pm 0.03 \text{ km}$  ( $\sim 100 \text{ m yr}^{-1}$ , 21%) (Figures 3(b) and 4(b)). The front of Horcones glacier advanced approximately  $3.1 \text{ km} \pm 0.06 \text{ km}$  ( $\sim 37.4\%$ ) at a  $1030 \text{ m yr}^{-1}$  rate in the 2002–2005 surge.

Among the newly identified surge events, Colina glacier had the most relevant one (Figures 4(c) and 5(a)). A strong advance of  $1 \text{ km}$  took place between 1967 and 1976 (35%,  $110 \text{ m yr}^{-1}$ ), whereas a second  $\sim 0.4 \text{ km}$  advance occurred between 2004 and 2013. Sierra Bella glacier advanced  $\sim 0.8 \text{ km}$  (25%,  $23 \text{ m yr}^{-1}$ ) from 1998 to 2012. Noticeable relative advances of  $\sim 10\%$  occurred in the Marmolejo ( $1 \text{ km}$ ,  $71 \text{ m yr}^{-1}$ ) during the 1962–1976 surge (Figures 3(d)

and 4(d)) and in the Grande del Juncal glacier ( $\sim 0.9 \text{ km}$ ,  $74 \text{ m yr}^{-1}$ ) between 1962 and 1974. These surges in the 1960s produced more prominent advances than in the 2000s on these glaciers (Table 2).

As for the remaining glaciers, the absolute and relative advance rates were considerably lower, including those six glaciers firstly identified as surge-type (Table 2). Because of the minor absolute and relative advances and the slow (close to  $10 \text{ m yr}^{-1}$ ) advance rates, we classified Colina Sur, Barroso, Oeste del Cerro Alto, Sierra Bella, Excelsior, and Loma Larga glaciers as index = 3 (possible surge-type).

Four of the sampled glaciers (Río Museo, Universidad, Juncal Sur, and Nieves Negras) have not advanced during our observation period (Table 2). Polleras glacier was effectively advancing in the mid-1980s, though the coarse resolution of the Landsat scenes, the extensive debris cover and the narrowness of the glacier tongue prevented a reliable estimation of the glacier advance.

## 3 Elevation and mass changes

We found that in the 2000–2011 period seven glaciers (Barroso, Cachapoal, Grande del Juncal, Sierra Bella, Laguna, Río Museo, Polleras) had an overall positive elevation or mass change, another seven have thinned or lost mass (Colina, Horcones, Oeste del Cerro Alto, Tunuyan, Universidad, Juncal Sur, Nieves Negras) whilst for the remaining five glaciers (Colina Sur, Marmolejo, Excelsior, Loma Larga, Plomo) the area-averaged mass balance has remained close to zero (Table 2). Overall, the surge-type glaciers showed very heterogeneous behavior with strongly negative to highly positive elevation change rates. Cachapoal glacier had the highest, positive average elevation change of  $1.01 \pm 0.31 \text{ m yr}^{-1}$ . The thickening rate is increased to  $1.45 \pm 0.31 \text{ m yr}^{-1}$  if only the active tongue is considered in the calculation (Figures 4(b) and 5(e)). A similar

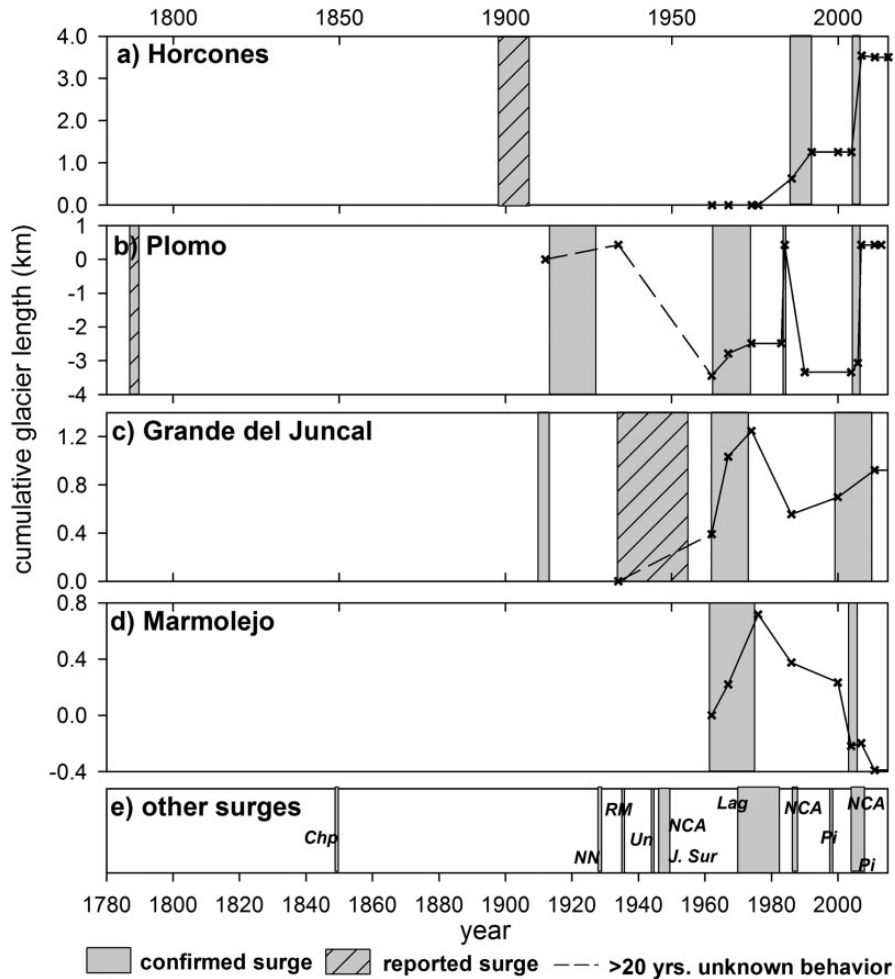


**Figure 3.** (a–d) Examples of repeated surges and length changes of surge-type glaciers in comparison with other confirmed surge events in the Central Andes. The black crosses represent terrain and/or remote sensing observations. The dashed lines link observed glacier frontal positions separated in time for more than 20 years. Within those periods, retreat/advance of the glacier is unknown. Abbreviations: Chp = Cachapoal; NN = Nieves Negras; RM = Río Museo; Un = Universidad; J. Sur = Juncal Sur; Lag = Laguna; Pi = Piuquenes; NCA = Noreste del Cerro Alto.

configuration of an inactive glacier tongue below the active one, though with a much lower rate of elevation change, was found for Colina Sur ( $-0.02 \pm 0.22$  m yr $^{-1}$ ), Loma Larga ( $-0.11 \pm 0.27$  m yr $^{-1}$ ), and Barroso ( $0.31 \pm 0.27$  m yr $^{-1}$ ).

In general, glaciers with the most prominent terminus advances have shown the strongest

thinning rates and more negative mass balances (Figure 5) (e.g. Horcones  $-0.48 \pm 0.38$  m w.e. yr $^{-1}$ ; Colina  $-0.37 \pm 0.24$  w.e. yr $^{-1}$ ). Thinning rates are predictably strong also on a number of glaciers that have surged prior to our study period (Universidad  $-0.56 \pm 0.30$  m yr $^{-1}$ ; Juncal Sur  $-1.08 \pm 0.27$  m yr $^{-1}$ ). Apart from the few highly thinning and thickening glaciers, the elevation

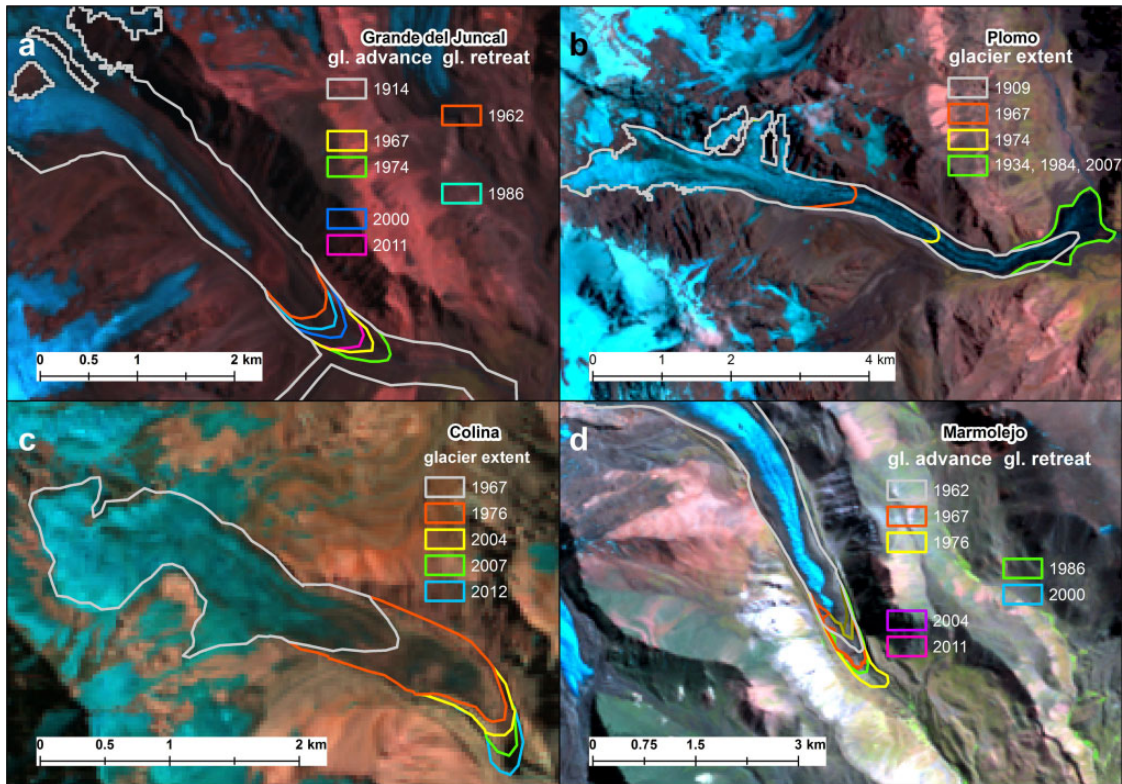


**Figure 4.** Frontal variations for (a) Grande del Juncal, (b) Plomo, (c) Colina, and (d) Marmolejo glaciers. Background images are Landsat scenes from the year 2000.

changes of the remaining fourteen glaciers had a more moderate trend, between  $\pm 0.3 \text{ m yr}^{-1}$ .

In the case of Tunuyan glacier ( $-0.30 \pm 0.33 \text{ m yr}^{-1}$ ), most of the elevation losses took place in the reservoir zones of the Piuquenes ( $-28.3 \text{ m}$ ) and Noreste del Cerro Alto tributaries ( $-14.2 \text{ m}$ ), but also in the portions in between the Noreste del Cerro Alto and Piuquenes receiving zones (which in turn show elevation gains of  $+19.6 \text{ m}$  and  $+14.0 \text{ m}$ ), in the northern tributary and in the glacier terminus (Figures 2 and 5(c)©). Elevation changes in the reservoir and receiving areas of Piuquenes and Noreste del Cerro Alto glaciers varied greatly in comparison with, Horcones ( $-1.8 \text{ m}$ ,  $+6.5 \text{ m}$ ), Plomo ( $-32.2 \text{ m}$ ,  $+30.9 \text{ m}$ ), and Colina ( $-10.2 \text{ m}$ ,  $+14.86 \text{ m}$ ).

#### 4 Surface velocities during the 1980s and 2000s Noreste del Cerro Alto and Piuquenes surges

The velocity of the glacier in the quiescent phase, as measured through March 2001–March 2002, was  $0.07 \pm 0.22 \text{ m d}^{-1}$ . The glacier began then to accelerate, the velocity increasing up to  $0.18 \pm 0.19 \text{ m d}^{-1}$  in the reservoir area between March 2002 and February 2003 (Figure 6(i)). Maximum velocities of  $2 \pm 1.1 \text{ m d}^{-1}$  (i.e., 28 times the velocity of the quiescent phase) were reached in the summer of 2004 (Figure 6(g)), when the surge wave was still in the reservoir area. Velocities averaged  $0.43 \text{ m d}^{-1}$  between March 2004 and January 2005, before a peak of  $\sim 3 \pm 1.9 \text{ m d}^{-1}$  ( $1.3 \pm 1.9 \text{ m d}^{-1}$  on average)

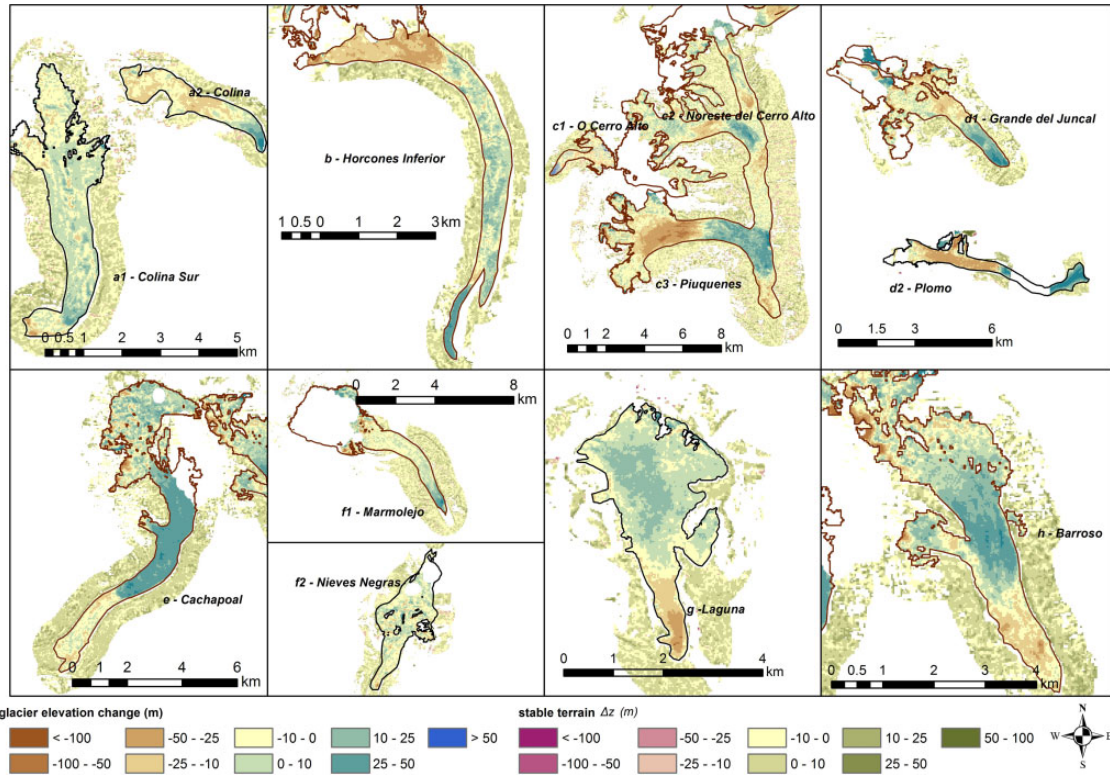


**Figure 5.** Examples of 2000–2011 elevation changes of thirteen glaciers. Elevation change is also illustrated in the buffer areas of stable terrain around glaciers. Glacier outlines are shown in black lines. White areas represent no data values. (a1) Colina Sur; (a2) Colina; (b) Horcones Inferior; (c1) Oeste del Cerro Alto; (c2) Noreste del Cerro Alto; (c3) Piuquenes; (d1) Grande del Juncal; (d2) Plomo; (e) Cachapoal; (f1) Marmolejo; (f2) Nieves Negras; (g) Laguna; (h) Barroso.

was measured in January–February 2005 (Figure 6(h)), as the surge front reached the limit of the main glacier valley. The February 2005–January 2006 time period shows a still surging, yet slowed down glacier (average  $0.63 \text{ m d}^{-1}$ ), whereas roughly similar velocities were also measured in January–February 2006. Additional Landsat imagery from February 2006 to March 2007 depicts a decelerated glacier flowing at max  $0.31 \text{ m d}^{-1}$  in the main glacier branch. By the summer of 2007 the glacier had entered its quiescent stage again ( $0.16 \text{ m d}^{-1}$ ) (Figure 6(i)).

Unlike Piuquenes glacier, Noreste del Cerro Alto surged in the mid-1980s. Although the initiation of this surge cannot be traced due to the unavailability of Landsat images from 1985,

the surge wave of Noreste del Cerro Alto had already entered the main Tunuyan glacier by February 1986 at a velocity of  $0.9 \pm 1.1$  (max  $3.1 \pm 1.1 \text{ m d}^{-1}$ ), and a maximum of  $1.8 \text{ m d}^{-1}$  in April of that year (Figure 6(a) and (c)). Velocities during the April 1986–February 2007 period show reduced velocities (max  $0.42 \text{ m d}^{-1}$ ). Shortly afterwards, the glacier decelerated rapidly and had slowed down to quiescent velocities (mean  $0.1 \text{ m d}^{-1}$ ) as measured in the summer of 1987 (Figure 6(c)).

The timing of the most recent Noreste del Cerro Alto surge was similar to the contemporary surge of Piuquenes glacier. Between 2001 and 2002, during the quiescent phase, the average glacier velocity was  $0.05 \pm 0.23 \text{ m d}^{-1}$  (i.e. a

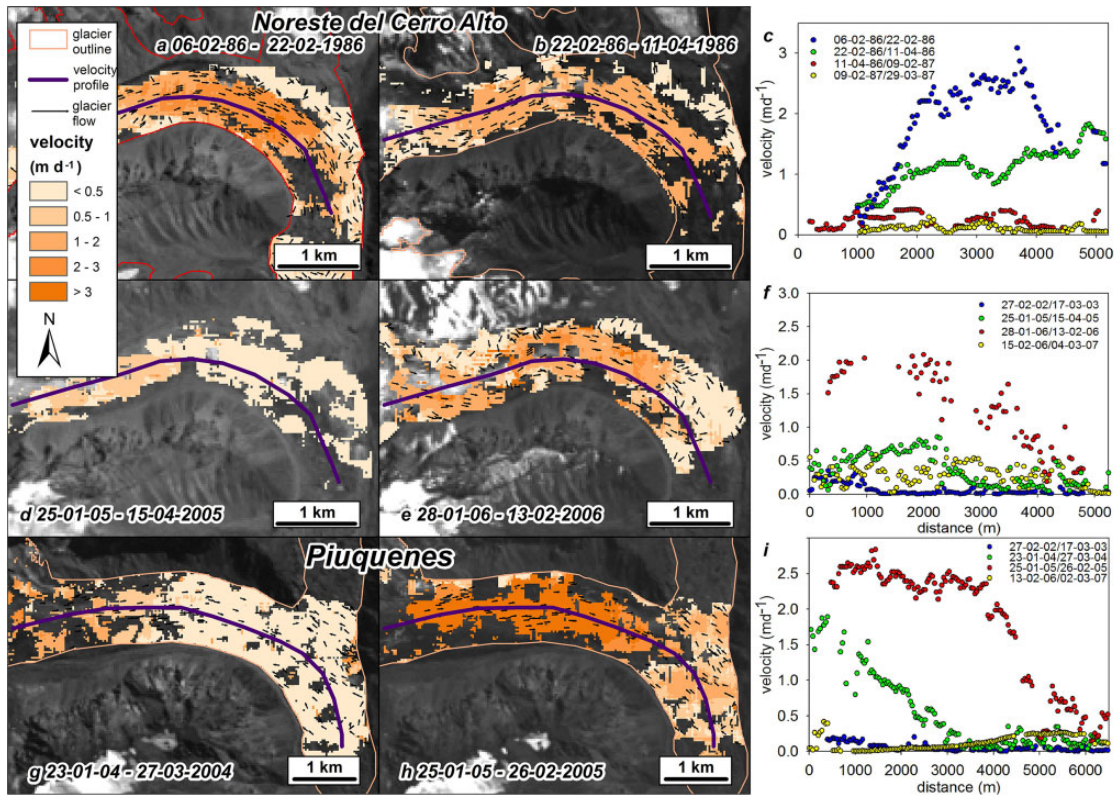


**Figure 6.** Glacier surface velocities during the active phases of the 1985–1987 (a-c) and 2003–2007 (d-f) Noreste del Cerro Alto surge. In both examples, the surge wave is captured in the reservoir area, with maximum velocities of  $3.1 \pm 1.1$  and  $\max 2 \pm 3.8 \text{ m d}^{-1}$ . (g-i) show the surge wave moving from the reservoir to the receiving area during the 2003–2007 Piuquenes surge ( $3 \pm 1.9 \text{ m d}^{-1}$ ).

velocity range between  $-0.18$  and  $0.28 \text{ m d}^{-1}$ . Velocities in the reservoir area had reached  $0.3 \pm 0.18 \text{ m d}^{-1}$  in the summer of 2003, and had slowly increased to  $0.6 \text{ m d}^{-1}$  by 2005 (Figure 6(e)). Throughout this year the glacier accelerated and flowed at a maximum of  $1 \text{ m d}^{-1}$ , peaking at  $2 \text{ m d}^{-1}$  in February 2006 (Figure 6(d) and (e)). By January 2007 velocities had decreased again to  $0.55 \text{ m d}^{-1}$ , and to quiescent velocities in early March.

## VI Discussion

### *I Length changes*

It is generally accepted (e.g. Bhattacharya et al., 2016; Bolch et al., 2012, WGMS, 2008) that

glacier length represents a delayed signal to climate change and is hard to interpret in climate terms. In particular, length changes of surge-type glaciers may not be directly related to climate (Jiskoot, 2011). There is at present no consensus in the literature about the absolute or relative magnitude of glacier terminus advances to qualify as a surge (Mukherjee et al., 2017). Based on the interpretation of the Landsat imagery, we found that slight glacier advances (normally in the order of a few dozen meters) were common in the study area during the second half of the 80's, (including some of the sampled surge-type glaciers such as Polleras, Oeste del Cerro Alto, Grande del Juncal, Marmolejo), when climate conditions were supposedly

favorable (Masiokas et al., 2016). Similarly, Universidad glacier, one of the largest of the investigated surge-type glaciers, advanced  $\sim 140$  m during that same period (Wilson et al., 2016). The  $\sim 0.4$  km advance of Nieves Negras around this time is the most prominent one among the investigated glaciers here. Throughout the 2000s, conditions were mostly unfavorable and glaciers retreated significantly on a regional scale in the Central Andes (Espizua and Pitte, 2009; Malmros et al., 2016; Masiokas et al., 2009). Yet, the newly identified possible surge-type glaciers had advances of up to 700 m (Table 2), which are undoubtedly larger than those in the 80's. In view of the above, and in addition to the glacier mass balance trends discussed above, we are confident that the small advances observed by us are minor surge episodes and not a normal response to climate variability.

When revisiting Innominado glacier, we found a discrepancy with the data presented by Llorens and Leiva (1995). These authors reported a 2.9 km advance of Innominado glacier between 1986 and 1991. We reassessed this advance to be around 1 km (i.e. probably a case of visual misinterpretation of the debris-covered ice extent) and observed that the core of the glacier advance took place between 1988 and 1989, and that by 1990 the glacier had become largely stable. No further advances were to be found.

## 2 Glacier mass balance records in the Central Andes

Glacier trends in the Central Andes have been that of steady and increasingly faster retreat since the second half of the 20th century (Bown et al., 2008; Malmros et al., 2016). Interspersed in the glacier record available in the region, however, periods of glacier advance and positive mass balance exist. The glacier with the longest mass balance record, Echaurren Norte, sustained positive mass balance conditions

during the entire 1980 decade and also during short-lived periods in the early 2000s (Masiokas et al., 2016). This is in coincidence with the nearby Piloto Este (Leiva et al., 2007) and Las Vacas (Lenzano, 2013) glaciers. Also Universidad glacier has undergone frontal advances and velocity increases that are roughly synchronous with these positive mass balance periods (Wilson et al., 2016). Nevertheless, and in general terms, glaciers in the Central Andes have been steadily thinning in recent years ( $-0.24 \pm 0.31$  m  $\text{yr}^{-1}$  – Falaschi et al., 2018;  $-0.77 \pm 0.22$  m  $\text{yr}^{-1}$  – Mernild et al., 2015).

During the second half of the 2000s, when glaciers in the area sustained a negative mass balance trend and thinned consequently (Mernild et al., 2015; Masiokas et al., 2016), the newly identified possible surge-type glaciers Barroso, Sierra Bella and Colina Sur glaciers had positive to  $\sim 0$  elevation changes or mass budgets, whilst Loma Larga and Oeste del Cerro Alto had only slightly negative elevation changes. This trend of slight glacier thickening or thinning is considerably mellow than the one found by Mernild et al. (2015), who correlated the imbalance of the glaciers in the Central Andes to the El Niño Southern Oscillation and the Pacific Decadal Oscillation. Some glaciers that have not surged since the first half of the twentieth century, such as Universidad and Juncal Sur, have also shrunk considerably in the last decade or so (Masiokas et al., 2009). The limited available elevation change data for Universidad ( $-0.56$  m  $\text{yr}^{-1}$ ) and Juncal Sur ( $-1.08$  m  $\text{yr}^{-1}$ ), would nonetheless suggest much higher thinning rates in comparison with the other surge-type glaciers in the area, much in agreement with the reported glacier-climate trends of Mernild et al. (2015).

## 3 Mass balance and elevation changes of surge-type glaciers

Our mass budget estimations showed that all of the glaciers whose terminus advanced between

2000 and 2011 have had negative to slightly positive mass balances during that time span (Table 2). These results are in agreement with the findings of Pieczonka and Bolch (2015), Mukherjee et al. (2017), and Gardelle et al. (2013), who suggested that the net mass balance of a surging glacier might be either negative or positive but in general closer to zero.

The timing of a glacier surge, relative to the analyzed time period for retrieving mass and elevation changes, influences the overall mass budget and thinning/thickening signal. Glaciers with a surge event fully enclosed in the 2000–2011 period (e.g., Marmolejo, Tunuyan, Oeste del Cerro Alto) had negative to  $\sim 0$  average elevation and mass changes. Because the study period incorporates the quiescent phase which follows surge termination, the mass budget calculation is probably biased towards enhanced thinning. In contrast, glaciers with post-2011 culminating surges (Barroso, Colina, and Sierra Bella) tend to have more positive mass budgets, as the mass transfer and elevation losses in the receiving area are not fully captured and surge termination occurs after the 2000–2011 study period.

The above is well exemplified in the case of Horcones glacier. Between February 2000 and March 2011, Horcones thinned at  $-0.56 \pm 0.33$  m yr<sup>-1</sup> on average, leading to an overall mass balance of  $-0.48 \pm 0.36$  m w.e. yr<sup>-1</sup>. The reservoir area thinned 21.8 m, whereas the receiving zone underwent an elevation change of 6.5 m on average. Pitte et al. (2016) calculated glacier elevation changes in the much shorter period between March 2003 and April 2004, at the peak of the active phase, and found a glacier thinning of  $-43 \pm 6$  m and a thickening of  $30 \pm 6$  m in the reservoir and receiving areas, respectively. Previously, Lenzano et al. (2013) had reported a total elevation change of  $23 \pm 10$  m by analyzing ASTER DEMs between 2001 and 2008. These differences probably arise from the difference in the analyzed time periods and the glacier processes that took place following

the surge. As the Horcones flow became nearly stagnant and entered the quiescent phase, the ice surface in the receiving area lowered and the glacier thinned. An average elevation decrease of  $0.8$  m d<sup>-1</sup> ( $\sim 2.9$  m yr<sup>-1</sup>) was measured between 2009 and 2014 (Lenzano et al., 2016). The  $>3$  km advance of Horcones meant that the glacier tongue was now laying at a much lower elevation, where the temperatures are warmer and ice is more prone to melt (Lenzano et al., 2016). After a surge, a glacier's ablation area is increased, causing a negative effect on mass balance (Oerlemans and van Pelt, 2015).

Positive elevation changes are widespread in the accumulation area of Laguna glacier (Figure 5(g)), whereas the lowermost part of the glacier is thinning and the tongue rapidly retreating. This might in fact illustrate the *buildup* phase, as the ice mass increases in the reservoir area before the active phase is initiated (Jiskoot, 2011), and may be indicative of the next surge of Laguna glacier.

#### 4 Glacier surface velocities

We recorded maximum velocities of  $3 \pm 1.9$  m d<sup>-1</sup> and  $3.5 \pm 1.2$  m d<sup>-1</sup> for Piuquenes and Noreste del Cerro Alto glaciers during the presumed peak (February 2005) of the 2003–2007 surge, whereas the maximum speed ( $3.1 \pm 1.1$  m d<sup>-1</sup>) of the 1985–1987 Noreste del Cerro Alto surge showed similar velocities in comparison with the 2003–2007 one. Quincey and Luckman (2014) have shown that surge characteristics such as velocities may vary among nearby individual glaciers within a surge-type glacier cluster to a large extent. Compared to the maximum  $14$  m d<sup>-1</sup> surface velocities measured at the peak (April 2004) of the Horcones 2002–2005 and  $35$  m d<sup>-1</sup> of the 2004–2007 Plomo surges (Pitte et al., 2016), both Piuquenes and Noreste del Cerro Alto have flown at much lower rates. These higher velocities in the Horcones and Plomo glaciers might stem from their topographical setting and morphological characteristics.



In order to transfer a given amount of ice volume in the particularly narrow gorge through which Horcones and Plomo flow, a faster flow is required in comparison to the broader Piuquenes and Noreste del Cerro Alto glacier valleys. Also, the larger areas, the gentler average slopes and the narrower elevation ranges possibly promote a slower propagation of the glacier front in the case of Piuquenes and Noreste del Cerro Alto. The differences in glacier valley morphology may also explain the comparatively lower thinning and thickening in the Piuquenes (−28.3 m and 19.6 m) and Noreste del Cerro Alto (−14.2 m and 14.0 m) reservoir and receiving areas when compared to Horcones.

### 5 Timing and duration of the surge events

From our investigations, it can be safely assumed that Piuquenes surged in the mid-2000s, whereas Noreste del Cerro Alto did so in the mid-1940s, mid-1980s. and mid- 2000s. Based on these evidences, it can be argued that Noreste del Cerro Alto glacier may have a surge cycle of ~20-40 years. The reported 1997 surge of Piuquenes by Lliboutry (1999) is not visible in the 1996–1998 Landsat imagery). Most probably, a then recent surge was assumed after a personal communication (“*Nearby, the east glacier of Nevado de los Piuquenes was found to be surging in January 1997 (A. Aristarain, oral commun. – Lliboutry, 1999: 1142).* With no repeated surges, it is hence not possible to determine the duration of the Piuquenes surge cycle. For the Plomo glacier, considering also the occurrence of the catastrophic surge prior to 1934 (Espizua, 1986), we hypothesize a ~20–30 years surge cycle. Prieto (1986) suggested the occurrence of a surge Plomo prior to 1786, and proposed a longer 50 year quiescent phase for Plomo glacier. With the greatly coincident timing of the last two surges of Plomo and Horcones glaciers in mind, it is worth noting that the latter did not surge contemporarily to the 1962–1974 Plomo surge. In contrast, Grande del

Juncal (and Marmolejo, incidentally) did surge in the mid-1960s and mid-2000s at the same time as the Plomo episodes.

The velocity increases appear to be gradual in the latest Noreste del Cerro Alto and Piuquenes surges (Figure 6), and defining a precise initiation (and termination) date of the active phases is problematic. This situation is worsened by the scarcity of satellite images suitable for tracking glacier features, due to the frequent cloud cover and the abundance of seasonal snow on the glacier surface around the winter and spring time. We nevertheless suggest that the active phases of the Noreste del Cerro Alto and Piuquenes are relatively short (2–3 years), and analogous in duration (but temporarily shifted) to the latest Horcones 2002–2005 surge (Pitte et al., 2016). In comparison to the Noreste del Cerro Alto and Piuquenes surge episodes, the last two surges of Plomo glacier seem to have taken place during shorter periods. The 1984 surge had fully developed within a less than a year span (February to November), whereas the major advance of the glacier during the latest surge was completed between February 2006 and September 2007 (Pitte et al., 2016). Conversely, the comparatively minor (in linear advance) third surge episode of Plomo glacier took much longer (1962-1974) to complete (though the timing of surge termination is an estimate, as there are no in between images available).

To our knowledge, all of glacier surges reported for the first half of the twentieth century and earlier on lack precise details of the timing of the surge events. Therefore, it is hardly possible to precisely determine the timing and duration of surge cycles. A second constrain is the low frequency of remote sensing data before the second half of the twentieth century. The surge-type glaciers in the Mendoza catchment, including Horcones, Plomo, Grande del Juncal, Innominado, and Polleras glaciers, have been nevertheless visited on a very frequent basis since the eighteenth century (Prieto, 1986). The Plomo and nearby glaciers,

as well as the Tunuyan creek, have been also investigated regularly ever since the 1934 Plomo flood by governmental administration (e.g., Departamento Provincial de Irrigación de Mendoza) to generate stream flow forecasts, noticing no other evidences of sudden, large glacier advances.

## 6 Surge mechanism

The time of the year at which surges initiate and terminate has been linked to the underlying surge mechanism (see introduction section). Pitte et al. (2016) proposed the Alaska-type, hydrological model for the Horcones glacier, in view of the short duration of the active phase and the abrupt change in the velocity in the 2002–2005 surge. Initiation of the active phase of the last two surges, however, was determined to have occurred in January 2003 and between October 1984–January 1985, which coincide with the summer and spring-early summer in the Southern Hemisphere, respectively. Similarly, both Plomo surges in the mid-1980s and mid-2000s started in February (Pitte et al., 2016). In the case of Noreste del Cerro Alto and Piuquenes glaciers, and whilst the available imagery might not be exhaustive, the active phases of the surges also started during the summer months (2005 and 2004, respectively; see Figure 6). This information would point out to a common surge mechanism among these four glaciers. Surge initiation during summertime is nonetheless in disagreement with the hydrological switch model, which should imply initiation during wintertime, or at least when the amount of input meltwater is scarce (Jiskoot, 2011). Contrary to what was found in the Horcones and Plomo glaciers, whose shift from quiescent to surge velocities was abrupt (Pitte et al., 2016), the latest surges of Noreste del Cerro Alto and Piuquenes are characterized by an acceleration period lasting 2–3 years before the velocity peak is attained. Such behavior is

expected for thermally triggered (Svalbard-type) glaciers (Quincey et al., 2011).

Elucidating a surge mechanism based only on the interpretation and feature tracking of satellite imagery to derive surge velocities is not entirely satisfactory, because cloud cover and seasonal snow might limit the compilation of a dense time series critically. In addition, there is a limited amount of evidence that can be obtained from satellite imagery concerning water fluxes into the glacier bed and the thermal state of glacier. Moreover, Jiskoot (2011) has highlighted that no systematic and comprehensive assessment of the surge seasonality related to an unequivocal surge mechanism has been carried out so far at large (global) scale. The dissimilar results presented here clearly show that this relation might not be straightforward, and more research must yet be conducted in the Andes. A conclusive assessment of the involved surge mechanisms should require in-situ, detailed data about the thermal state of glacier beds and the characteristics of the subglacial drainage systems in the sampled glaciers.

## 7 Comparison with other regions with focus on the Karakorum

Among the various glacier clusters around the Globe (e.g., Greenland, Svalbard, Arctic Canada), the Karakorum Range in Asia, which hosts a large number (>160) of surging glaciers (Bhambri et al., 2017), presents several climate features that bear the greatest resemblance to the Central Andes, an assertion already made by Helbling (1935). The high aridity, wide thermal amplitude, high solar radiation and strong winds, all contribute to the formation of extensive debris covers on glaciers in a similar climatic environment. With some reservations, Sevestre and Benn (2015) have argued that all major surge-type glacier clusters are exposed to colder and drier climate conditions. On the other hand, several surge-type glaciers (e.g., Svalbard, Alaska, and East Greenland) are much

larger in size compared to the Andean cluster. In fact, from the surging glacier data in Sevestre and Benn (2015), we found that except for the surge-type glaciers in the Caucasus, the Central Andes surge-type glacier cluster contains in general the smallest glaciers worldwide. Whilst we do not rule out comparisons with glacier clusters other than the Karakorum, we made focus on this latter site.

Regarding glacier length changes and probably because of the much smaller size, the length changes of the glaciers here investigated may seem of little relevance in comparison to the extraordinary surges in the Karakorum, where advances of several kilometers are common (e.g. Copland et al., 2011; Paul, 2015; Quincey and Luckman, 2014). In their thorough review of Karakorum glacier surges, Bhambri et al. (2017) report the 12 km and 10 km advances of Khutia and Hassanabad glaciers, which are 3–4 times greater than the  $\sim 3$  km advances of Horcones and Plomo surges. Initial glacier size is nevertheless not necessarily related to the magnitude of the surge advance. The 220 km<sup>2</sup> and 65 km long Lowell glacier in the Yukon, for example, advanced 2.85 km in its latest surge (Bevington and Copland, 2014), an extent similar to the much smaller and shorter Horcones or Plomo glaciers. For the small surge-type glaciers in the Central Andes, similar relative length changes compared to larger glaciers elsewhere (e.g. Mukherjee et al., 2017) may be of equal relevance. We hypothesize that the rather small advances of the surge-type glaciers of the Central Andes have hampered the proper identification of a larger number. The smaller magnitude of glacier surges, the limited size of geomorphologic features and inadequate temporal imagery resolution make the glaciers more difficult to identify based purely on the interpretation of satellite imagery.

In terms of glacier velocities during glacier surges, measurements on a large number of glaciers in the Karakorum reveal slow, generally  $<6$  m d<sup>-1</sup> velocities (Quincey and Luckman,

2014; Quincey et al., 2011, 2015; Rankl et al., 2014), much in concordance with the velocity values that we determined for Piuquenes and Noreste del Cerro Alto. Exceptionally, velocities of up to 400 m d<sup>-1</sup> have been documented for the Yengutz Har Glacier (Bhambri et al., 2017). In comparison to the large surge-type glaciers in Alaska-Yukon or Svalbard (see Bevington and Copland, 2014; Burgess et al., 2012; Dunse et al., 2015), the surface velocities of Piuquenes and Noreste del Cerro Alto appear much slower.

The analyzed data for the Plomo, Horcones, Noreste del Cerro Alto, and Piuquenes glaciers suggest that they all have short active phases separated by quiescent faces of a few decades. A number of surge-type glaciers in the Karakorum have shown repeated, frequent surges in relatively short time periods (Paul, 2015; Quincey and Luckman, 2014). In the Pamir, Medvezhiy Glacier surged 5 times between 1963 and 2011 (Osipova, 2015). On the contrary, some of the sampled glaciers did not surge since the early 20th century (e.g. Universidad, Río Museo, Nieves Negras, Juncal Sur). A flood released in 1848 from Cachapoal glacier (Plagemann, 1887) was interpreted as a glacier surge by Rothlisberger (1986). More floods followed in 1955 and 1981 (Iturrizaga and Charrier, 2013), though a direct relation with glacier surges has not been firmly acknowledged. At least for the second event, we were unable to identify any surge evidences from remote sensing data. The absence of repeated surges on them would suggest relatively longer surge cycles common amongst them. This is indeed interesting, as such long quiescent phases have been described for the higher latitude surging glaciers in Svalbard, Greenland, and Alaska (Jiskoot and Juhlin 2009; Jiskoot et al., 1998; Kienholz et al., 2017). The dissimilar duration of the quiescent phases found in the Central Andes has been also observed for glacier surges in the Karakorum (Quincey et al., 2015).

## VII Conclusions

On the basis of aerial photographs, medium- to high resolution satellite imagery and DEM differencing, we have identified 21 surge-type glaciers in the Central Andes of Argentina and Chile, from which six glaciers were here identified for the first time as possible surge-type glaciers. In addition, 11 new surge episodes were identified among these glaciers. The present study constitutes hence the most up-to date and detailed surge-type inventory of this particular region of the Andes so far.

Advance rates of the investigated surge-type glaciers were found to be highly dissimilar, Colina glacier having shown the greatest advance from the newly identified surge events. Glaciers that advanced in the 2000–2011 study period showed negative to slightly positive mass balance conditions, relating to the timing of the surge events and not necessarily in accordance with the wider, regional trend of moderate to high thinning rates.

The few available surveys for surge-type glaciers in the Central Andes reveal variable velocities during surges (up to one order of magnitude), though fairly slower compared with recorded velocities in high-latitude surge-type glacier clusters. The Piuquenes and Nor-este del Cerro Alto velocity change between the quiescent and the surge phase was estimated to be ~40–50 times faster during the 2003–2007 surge event. Whilst repeated surges for five glaciers allowed for the estimation of surge cycles of ~20–40 years, the remaining glaciers have not surged since the first half of the twenty-first century or have only done so in recent years, and may have longer quiescent phases with >50 years cycles, which would in turn suggest heterogeneous duration of the surge cycles.

On average, surge-type glaciers in the Central Andes are much smaller in size and have shown minor absolute advances compared to most major surge-type clusters in the World, though relative advances can be of comparable

magnitude among surge-type glaciers of different size. Also, the velocities during glacier surges in the Central Andes are consistently lower in comparison with velocities recorded in high-latitude surge-type glacier clusters, though they resemble velocities often found in the Karakorum. Similar characteristics between surge-type glaciers in the Central Andes and the Karakorum include also the variable duration of surge cycles and possibly, the dissimilar underlying surge mechanisms within a single glacier cluster.

## Acknowledgements

The DEM co-registration tool was downloaded from Etienne Berthier's personal homepage at <http://etienne.berthier.free.fr/> Special thanks to the Japan Aerospace exploration Agency (JAXA) for freely providing the ALOS data sets and to the Argentinean National Glacier Inventory initiative ([www.glaciar-esargentinos.gob.ar](http://www.glaciar-esargentinos.gob.ar)) for the glacier inventory data. Thanks also to Juan Antonio Rivera, Rafael Bottero, (IANIGLA), Sebastián Cisternas and Claudio Bravo (Centro de Estudios Científicos, Chile) and Estela Rusconi from SEGEMAR. Finally, we are thankful to PPGE Managing Editor Nick Clifford and two anonymous reviewers for their guidance and contributions in the review process of the original text, which was fundamental for a much improved presentation of this study's content.


## Declaration of Conflicting Interests

The author(s) declared no potential conflicts of interest with respect to the research, authorship, and/or publication of this article.

## Funding

The author(s) received no financial support for the research, authorship, and/or publication of this article.

## ORCID iD

Daniel Falaschi  <http://orcid.org/0000-0001-9232-2813>

## References

- Barrand NE and Murray T (2006) Multivariate controls on the incidence of glacier surging in the Karakoram Himalaya. *Arctic, Antarctic and Alpine Research* 38(4): 489–498.
- Benn DI and Evans DJA (2010). *Glaciers and Glaciation*. 2nd ed. London: Hodder Education.
- Berthier E, Arnaud Y, Rajesh K, et al. (2007) Remote sensing estimates of glacier mass balances in the Himachal Pradesh (Western Himalaya, India). *Remote Sensing of Environment* 108(3): 327–338.
- Berthier E, Raup B and Scambos T (2003) New velocity map and mass-balance estimate of Mertz Glacier, East Antarctica, derived from Landsat sequential imagery. *Journal of Glaciology* 49(167): 503–511.
- Berthier E, Vadon H, Baratoux D, et al. (2005) Surface motion of mountain glaciers derived from satellite optical imagery. *Remote Sensing of Environment* 95(1): 14–28.
- Bevington A and Copland L (2014) Characteristics of the last five surges of Lowell Glacier, Yukon, Canada, since 1948. *Journal of Glaciology* 60(219): 113–123.
- Bhambri R, Hewitt K, Kawishwar P, et al. (2017) Surge-type and surge-modified glaciers in the Karakorum. *Scientific Reports* 7(1): 15391.
- Bhattacharya A, Bolch T, Mukherjee K, et al. (2016) Overall recession and mass budget of Gangotri Glacier, Garhwal Himalayas, from 1965 to 2015 using remote sensing data. *Journal of Glaciology* 62(236): 1115–1133.
- Bolch T, Menounos B and Wheate R (2010). Landsat-based inventory of glaciers in western Canada, 1985–2005. *Remote Sensing of Environment* 114: 127–137.
- Bolch T, Kulkarni A, Kääb A, et al. (2012) The state and fate of Himalayan glaciers. *Science* 336: 310–314.
- Bolch T, Pieczonka T, Mukherjee K, et al. (2017) Glaciers in the Hunza Catchment (Karakoram) are almost in balance since the 1970s. *The Cryosphere* 11: 531–539.
- Bown F, Rivera A and Acuña C (2008). Recent glacier variations at the Aconcagua basin, central Chilean Andes. *Annals of Glaciology* 48: 43–48.
- Bruce RH, Cabrera GA, Leiva JC, et al. (1987) The 1985 surge and ice dam of Glacier Grande del Nevado del Plomo, Argentina. *Journal of Glaciology* 33(113): 131–132.
- Burgess EW, Forster RR, Larsen CF, et al. (2012) Surge dynamics on Bering Glacier, Alaska, in 2008–2011. *The Cryosphere* 6: 1251–1262.
- Casassa G, Espizua LE, Francou B, et al. (1998) Glaciers in South America. In: Haeberli W, Hoelzle M and Soter S (eds) *Into the Second Century of Worldwide Glacier Monitoring: Prospects and Strategies*. Studies and Reports in Hydrology 56. Paris: UNESCO, 125–146.
- Cobos D and Boninsegna J (1983). Fluctuations of some glaciers in the upper Atuel River basin, Mendoza, Argentina. In: Balkema AA (ed) *Quaternary of South America and Antarctic Peninsula*. Rotterdam: Balkema, 61–82.
- Condom T, Coudrain A, Sicart JE, et al. (2007) Computation of the space and time evolution of equilibrium-line altitudes on Andean glaciers (10°N–55°S). *Global and Planetary Change* 59: 189–202.
- Copland L, Sharp MJ and Dowdeswell JA (2003) The distribution and flow characteristics of surge-type glaciers in the Canadian High Arctic. *Annals of Glaciology* 36(1): 73–81.
- Copland L, Sylvestre T, Bishop MP, et al. (2011) Expanded and recently increased glacier surging in the Karakoram. *Arctic, Antarctic and Alpine Research* 43(4): 503–516.
- Cox P, Goudge K, Longstaff TG, et al. (1935) The Study of Threatening Glaciers: Discussion. *The Geographical Journal* 85(1): 36–41.
- Dehecq A, Millan R, Berthier E, et al. (2016) Elevation changes inferred from TanDEM-X data over the Mont-Blanc area: impact of the X-band interferometric bias. *IEEE Journal of Selected Topics and Applied Earth Observations and Remote Sensing* 9(8A): 3870–3882.
- Dowdeswell JA, Hamilton GS and Hagen JO (1991) The duration of the active phase on surge-type glaciers: contrasts between Svalbard and other regions. *Journal of Glaciology* 37(127): 338–400.
- Dunse T, Schellenberger T, Hagen JO, et al. (2015) Glacier-surge mechanisms promoted by a hydrothermodynamic feedback to summer melt. *The Cryosphere* 9: 197–215.
- Espizua LE (1986) Fluctuations of the Rio del Plomo Glaciers. *Geografiska Annaler* 68A(4): 317–327.
- Espizua LE (1987) Fluctuaciones de los glaciares del Río del Plomo, Mendoza. *Revista de la Asociación Geológica Argentina* 42(1–2): 112–121.
- Espizua LE and Bengochea JD (1990) Surge of Grande del Nevado Glacier (Mendoza, Argentina) in 1984: Its evolution through satellite images. *Geografiska Annaler Series A, Physical Geography* 72(3/4): 255–259.
- Espizua LE and Pitte P (2009) The Little Ice Age glacier advance in the Central Andes (35°S), Argentina. *Palaeogeography, Palaeoclimatology, Palaeoecology* 281: 345–350.

- Falaschi D, Masiokas M, Tadono T, et al. (2016) ALOS-derived glacier and rock glacier inventory of the Volcán Domuyo region ( $\sim 36^\circ$  S), southernmost Central Andes, Argentina. *Zeitschrift für Geomorphologie* 60(3): 195–208.
- Falaschi D, Bolch T, Rastner P, et al. (2017) Mass changes of alpine glaciers at the eastern margin of the Northern and Southern Patagonian Icefields between 2000 and 2012. *Journal of Glaciology* 63(238): 258–272.
- Falaschi D, Lenzano MG, Tadono T, et al. (2018) Balance de masa geodésico 2000–2011 de los glaciares de la Cuenca Del Río Atuel, Andes Centrales de Mendoza (Argentina) *Geoacta* 42(2): 7–22.
- Farr TG, Rosen PA, Caro E, et al. (2004) The shuttle radar topography mission. *Reviews of Geophysics* 45: RG2004.
- Fischer M, Huss M and Hoelzle M (2015) Surface elevation and mass changes of all Swiss glaciers 1980–2010. *The Cryosphere* 9: 525–540.
- Gardelle J, Berthier E, Arnaud Y, et al. (2013) Region-wide glacier mass balances over the Pamir-Karakoram-Himalaya during 1999–2011. *The Cryosphere* 7: 1263–1286.
- Garreaud RD (2009) The Andes climate and weather. *Advances in Geosciences* 7: 1–9.
- Grant KL, Stokes CR and Evans IS (2009) Identification and characteristics of surge-type glaciers on Novaya Zemlya, Russian Arctic. *Journal of Glaciology* 55(194): 960–972.
- Hall DK, Bahr KJ, Shoener W, et al. (2003) Consideration of the errors inherent in mapping historical glacier positions in Austria from the ground and space. *Remote Sensing of Environment* 86(4): 566–577.
- Happoldt H and Schrott L (1993) Horcones Inferior-Glacier surge. In: *Fluctuations of Glaciers 1985–1990, Volume 6*. Zurich: IAHS (ICSU)/UNEP/UNESCO, 70.
- Harrison WD and Post AS (2003) How much do we really know about glacier surging? *Annals of Glaciology* 36: 1–6.
- Harrison WD, Osipova GB, Nosenko GA, et al. (2015) Glacier surges. In: Haerberli W, Whiteman C and Shroder JF (eds) *Snow and Ice-Related Hazards, Risks and Disasters*. Boston, MA: Academic Press, 437–485.
- Heid T and Käab A (2012) Evaluation of existing image matching methods for deriving glacier surface displacements globally from optical satellite imagery. *Remote Sensing of Environment* 118: 339–355.
- Helbling R (1919) *Beiträge zur Topographischen Erschliessung der Cordilleras de los Andes zwischen Aconcagua und Tupungato. XXIII*. Zürich: Jahresbericht des Akademischen Alpenclub Zürich.
- Helbling R (1935) The origin of the Rio Plomo ice-dam. *The Geographical Journal* 85(1): 41–49.
- Huss M (2013) Density assumptions for converting geodetic glacier volume change to mass change. *The Cryosphere* 7: 877–887.
- Iturrizaga L and Charrier R (2013) Glacialmorphological reconstruction of glacier advances and glacial lake outburst floods at the Cachapoal glacier in the Dry Central Andes of Chile ( $34^\circ$ S). In: *EGU General Assembly Conference Abstracts*, Vol. 15.
- Jiskoot H (2011) Glacier surging. In: Singh VP, Singh P and Haritashya UK (eds) *Encyclopedia of Snow, Ice and Glaciers*. Dordrecht, The Netherlands: Springer, 415–428.
- Jiskoot H and Juhlin DT (2009) Surge of a small East Greenland glacier, 2001–2007, suggests Svalbard-type surge mechanism. *Journal of Glaciology* 55(191): 567–570.
- Jiskoot H, Boyle P and Murray T (1998) The incidence of glacier surging in Svalbard: Evidence from multivariate statistics. *Computers & Geosciences* 24(4): 387–399.
- Käab A and Vollmer M (2000) Surface geometry, thickness changes and flow fields on creeping mountain permafrost: automatic extraction by digital image analysis. *Permafrost and Periglacial Processes* 11(4): 315–326.
- Käab A, Huggel C, Fischer L, et al. (2005a) Remote sensing of glacier- and permafrost-related hazards in high mountains: an overview. *Natural Hazards and Earth System Sciences* 5: 527–554.
- Käab A, Reynolds JM and Haerberli W (2005b) Glacier and permafrost hazards in high mountains. In: Huber UM, Bugmann HKM and Reasoner MA (eds) *Global Change and Mountain Regions. Advances in Global Change Research*, Vol. 23. Dordrecht, the Netherlands: Springer, 225–234.
- Kienholz C, Hock R, Truffer M, et al. (2017) Mass balance evolution of Black Rapids Glacier, Alaska, 1980–2100, and its implications for surge recurrence. *Frontiers in Earth Science* 5: 56.

- King WDVO (1934) The Mendoza River flood of 10–11 January 1934, Argentina. *The Geographical Journal* 84(4): 321–326.
- King WDVO (1935) A further report on the Plomo Valley ice-dam, Argentina. *The Geographical Journal* 86(5): 441–444.
- Koblet T, Gärtner-Roer I, Zemp M, et al. (2010) Reanalysis of multi-temporal aerial images of Storglaciaren, Sweden (1959–99). Part 1. Determination of length, area, and volume changes. *The Cryosphere* 4: 333–343.
- Kumari S, Ghosh SK and Buchroithner MF (2014) Measurement of glacier velocity at Pik Lenin, Tajikistan, by feature tracking. In: *ISPRS Technical Commission VIII symposium*, Hyderabad, India, 9–12 December 2014, 531–536.
- Le Bris R and Paul F (2015) Glacier-specific elevation changes in western Alaska. *Annals of Glaciology* 56(70): 184–192.
- Leiva JC (2006) Assessment of climate change impacts on the water resources at the northern oases of Mendoza province, Argentina. In: Price MF (ed) *Global Change in Mountain Regions*. London: Sapiens Publishing, 343.
- Leiva JC, Cabrera GA and Lenzano LE (2007) 20 years of mass balances on the Piloto glacier, Las Cuevas river basin, Mendoza, Argentina. *Global and Planetary Change* 59: 10–16.
- Lenzano MG (2013) Assessment of using ASTER-derived DTM for glaciological applications in the Central Andes, Mt. Aconcagua, Argentina. *Photogrammetrie, Fernerkundung, Geoinformation* 3: 197–208.
- Lenzano MG, Leiva JC, Trombotto D, et al. (2011) Satellite images and geodetic measurements applied to the monitoring of the Horcones Inferior glacier, Mendoza, Argentina. *Geoacta* 36(1): 13–25.
- Lenzano MG, Lenzano L, Barón J, et al. (2016) Thinning of the Horcones inferior debris-covered glacier, derived from five ablation seasons by semi-continuous GNSS geodetic surveys (Mt. Aconcagua, Argentina). *Andean Geology* 43(1): 47–59.
- Lenzano MG, Lenzano L, Trombotto Liaudat D, et al. (2013) Applying GNSS and DTM technologies to monitor the ice balance of the Horcones Inferior glacier, Aconcagua Region, Argentina. *Journal of the Indian Society of Remote Sensing* 41(4): 969–980.
- Lliboutry L (1956) *Nieves y glaciares de Chile, fundamentos de glaciología*. Santiago, Chile: Universidad de Chile, 472.
- Lliboutry L (1958) Studies of the shrinkage after a sudden advance, blue bands and wave ogives on Glaciar Universidad (central Chilean Andes). *Journal of Glaciology* 3(24): 261–270.
- Lliboutry L (1999) Glaciers of Chile and Argentina. In: Williams RS and Ferrigno JG (eds) *Satellite Image Atlas of Glaciers of the World. South America, Vol. 1386-I*. Denver, CO: U.S. Geological Survey.
- Llorens RE and Leiva JC (1995) Glaciological studies in the high Central Andes using digital processing of satellite images. *Mountain Research and Development* 15(4): 323–330.
- Malmros JK, Mernild SH, Wilson R, et al. (2016) Glacier area changes in the central Chilean and Argentinean Andes 1955–2013/14. *Journal of Glaciology* 62(232): 391–401.
- Masiokas M, Christie DA, Le Quesne C, et al. (2016) Reconstructing the annual mass balance of the Echaurren Norte glacier (Central Andes, 33.5° S) using local and regional hydroclimatic data. *The Cryosphere* 10: 927–940.
- Masiokas MH, Rivera A, Espizua LE, et al. (2009) Glacier fluctuations in extratropical South America during the past 1000 years. *Palaeogeography, Palaeoclimatology, Palaeoecology* 281: 242–268.
- Masiokas MH, Villalba R, Christie DA, et al. (2012) Snowpack variations since AD 1150 in the Andes of Chile and Argentina (30°–37°S) inferred from rainfall, tree-ring and documentary records. *Journal of Geophysical Research* 117: D05112.
- Maurer S, Rupper B and Schaefer JM (2016). Quantifying ice loss in the eastern Himalayas since 1974 using declassified spy satellite imagery. *The Cryosphere* 10: 2203–2215.
- Meier MF and Post AS (1969) What are glacier surges? *Canadian Journal of Earth Sciences* 6(4): 807–817.
- Mernild SH, Beckerman AP, Yde JC, et al. (2015) Mass loss and imbalance of glaciers along the Andes Cordillera to the sub-Antarctic islands. *Global and Planetary Change* 133: 109–119.
- Milana JP (2004) Modelización de la deformación extensional ocasionada por el avance catastrófico (surge) del Glaciar Horcones Inferior, Mendoza, Argentina. *Revista de la Asociación Geológica Argentina* 59: 167–177.
- Milana JP (2010) Hielo y Desierto. *Los glaciares áridos de San Juan*. San Juan: Elite Ediciones.

- Mukherjee K, Bolch T, Goerlich F, et al. (2017) Surge-type glaciers in the Tien Shan (Central Asia). *Arctic, Antarctic, and Alpine Research* 49(1): 147–171.
- Nogami M (1972) The snow line and climate during the last glacial period in the Andes mountains. *The Quaternary Research (Japan)* 11: 71–80.
- Oerlemans J and van Pelt WJJ (2015) A model study of Abrahamsenbreen, a surging glacier in northern Spitsbergen. *The Cryosphere* 9: 767–779.
- Osipova GB (2015) Fifty years of studying the Medvezhiy Glacier (West Pamirs) by the Institute of Geography, RAS. *Ice and Snow* 9(1): 129–140.
- Paul F (2015) Revealing glacier flow and surge dynamics from animated satellite image sequences: examples from the Karakoram. *The Cryosphere* 9: 2201–2214.
- Paul F, Barrand NE, Baumann S, et al. (2013) On the accuracy of glacier outlines derived from remote sensing data. *Annals of Glaciology* 54(63): 171–182.
- Paul F, Kääb A, Maisch M, et al. (2002) The new remote-sensing-derived Swiss glacier inventory. I. Methods. *Annals of Glaciology* 34: 355–361.
- Pfeffer WT, Arendt AA, Bliss A, et al. (2014) The Randolph Glacier Inventory: a globally complete inventory of glaciers. *Journal of Glaciology* 60(221): 537–552.
- Pieczonka T and Bolch T (2015) Region-wide glacier mass budgets and area changes for the Central Tien Shan between ~1975 and 1999 using Hexagon KH-9 imagery. *Global and Planetary Change* 128: 1–13.
- Pitte P, Berthier E, Masiokas MH, et al. (2016) Geometric evolution of the Horcones Inferior Glacier (Mt. Aconcagua, Central Andes) during the 2002–2006 surge. *Journal of Geophysical Research: Earth Surface* 121: 111–127.
- Plagemann A (1887) Das andine Stromgebiet des Cachapoal. In: *Petermanns Geogr. Mitteilungen. Heft III*. Gotha, 65–82
- Prieto MR (1986) The glacier dam on Río Plomo: a cyclic phenomenon? *Zeitschrift für Gletscherkunde und Glazialgeologie* 22(1): 73–78.
- Quincey DJ and Luckman A (2014) On the magnitude and frequency of Khurdopin glacier surge events. *The Cryosphere* 8: 571–574.
- Quincey DJ, Braun M, Glasser NF, et al. (2011) Karakoram glacier surge dynamics. *Geophysical Research Letters* 38: L18504.
- Quincey DJ, Glasser NF, Cook SJ, et al. (2015) Heterogeneity in Karakoram glacier surges, *Journal of Geophysical Research. Earth Surface* 120: 1288–1300.
- Rankl M, Kienholz C and Braun M (2014) Glacier changes in the Karakoram region mapped by multimission satellite imagery. *The Cryosphere* 8: 977–989.
- Raymond CF (1987) How do glaciers surge? A review. *Journal of Geophysical Research* 92(B9): 9121–9134.
- RGI Consortium (2017) *Randolph Glacier Inventory – a dataset of global glacier outlines: version 6.0*. Technical report. Boulder, CO: Global Land Ice Measurements from Space.
- Rignot E, Echelmeyer K and Krabill W (2001) Penetration depth of interferometric synthetic-aperture radar signals in snow and ice. *Geophysical Research Letters* 28(18): 3501–3504
- Rivera A and Bown F (2013) Recent glacier variations on active ice capped volcanoes in the Southern Volcanic Zone (37°–46°S), Chilean Andes. *Journal of South American Earth Sciences* 45: 345–356.
- Rivera A, Bown F, Carrión D, et al. (2012) Glacier responses to recent volcanic activity in Southern Chile. *Environmental Research Letters* 7: 014036.
- Rolstad C, Haug T and Denby B (2009) Spatially integrated geodetic glacier mass balance and its uncertainty based on geostatistical analysis: application to the western Svartisen ice cap, Norway. *Journal of Glaciology* 55(192): 666–680.
- Rothlisberger F (1986) 10.000 Jahre Gletschergeschichte die Erde: ein Vergleich zwischen Nord und Sudhemisphäre Glacier fluctuations, Sauerlander.
- Round V, Leinss S, Huss M, et al. (2017) Surge dynamics and lake outbursts of Kyagar Glacier, Karakoram. *The Cryosphere* 11: 723–739.
- Sagredo EA and Lowell TV (2012) Climatology of Andean glaciers: a framework to understand glacier response to climate change. *Global and Planetary Change* 86–87: 101–109.
- Schellenberger A (2014) Robert Helbling – Pionier der Stereophotogrammetrie in den argentinischen Anden und in der Schweiz. *Cartographica Helvetica* 49: 15–26.
- Sevestre H and Benn DI (2015) Climatic and geometric controls on the global distribution of surge-type glaciers: implications for a unifying model of surging. *Journal of Glaciology* 61(228): 646–662.
- Sievers W (1903) *Süd- und Mittelamerika*. Leipzig: Bibliographisches Institut, 665.
- Smith T, Bookhagen B and Cannon F (2015) Improving semi-automated glacier mapping with a multi-method approach: applications in central Asia. *The Cryosphere* 9: 1747–1759.



- Takaku J and Tadono T (2009) PRISM on-orbit geometric calibration and DSM performance. *IEEE Transactions on Geoscience and Remote Sensing* 47(12): 4060–4073.
- Unger C, Espizúa LE and Bottero R (2000) Untersuchung von gletscherständen im Tal des Rio Mendoza (zentralargentinische Anden) - kartierung eines surgevorstosses des Horcones Inferior. *Zeitschrift für Gletscherkunde und Glazialgeologie* 36: 151–157.
- Weidick A (1988) Surging glaciers in Greenland: a status. *Rapport Grønlands Geologiske Undersøgelse* 140: 106–110.
- WGMS (2008) *Global Glacier Changes: Facts and Figures*. Zurich, Switzerland: WGMS/UNEP.
- WGMS (2017) *Fluctuations of Glaciers Database*. Zurich, Switzerland: World Glacier Monitoring Service.
- Wilson R, Mernild SH, Malmros JK, et al. (2016) Surface velocity fluctuations for Glaciar Universidad, central Chile, between 1967 and 2015. *Journal of Glaciology* 62(235): 847–860.
- Yde JC and Knudsen NT (2007) 20th-century glacier fluctuations on Disko Island (Qeqertarsuaq), Greenland. *Annals of Glaciology* 46: 209–214.
- Zemp M, Thibert E, Huss M, et al. (2013) Reanalysing glacier mass balance measurement series. *The Cryosphere* 7: 1227–1245.

## Appendix A

**Table A1.** List of all satellite and aerial photography data used for the study.

Acquisition date (mm-dd-yyyy)	Sensor	Spatial resolution (m)	Path/Row	Use
03-05-1967	Corona KH4A	~2.7	DS1039-2173DF041	glacier mapping
23-02-1967	Corona KH4A	~2.7	DS1039-1014DA014	glacier mapping
23-02-1967	Corona KH4A	~2.7	DS1039-1014DA015	glacier mapping
04-08-1962	Wild RC5	–	–	glacier mapping
04-?-1974	Wild RC5	–	–	glacier mapping
03-15-1976	Landsat MSS	60	249/083	glacier mapping
02-22-1986	Landsat TM	30	232/083	cross-correlation/glacier mapping
04-11-1986	Landsat TM	30	232/083	cross-correlation/glacier mapping
02-09-1987	Landsat TM	30	232/083	cross-correlation
03-29-1987	Landsat TM	30	232/083	cross-correlation
03-10-1992	Landsat TM	30	232/083	glacier mapping
02-14-1998	Landsat TM	30	233/083	glacier mapping
02-10-1999	Landsat TM	30	232/083	inventory check
02-10-1999	Landsat TM	30	232/084	inventory check
02-29-2000	Landsat TM	30	232/083	glacier mapping
01-28-2000	Landsat TM	30	232/084	glacier mapping
03-11-2001	Landsat ETM+	15	232/083	cross-correlation
02-27-2002	Landsat TM	30	232/083	cross-correlation
03-06-2002	Landsat TM	30	232/083	cross-correlation
03-17-2003	Landsat ETM+	15	232/083	cross-correlation
01-23-2004	Landsat TM	30	232/083	cross-correlation
03-27-2004	Landsat TM	30	232/083	cross-correlation
01-25-2005	Landsat TM	30	232/083	cross-correlation
02-26-2005	Landsat TM	30	232/083	cross-correlation
04-15-2005	Landsat TM	30	232/083	cross-correlation

(continued)

**Table A1.** (continued)

Acquisition date (mm-dd-yyyy)	Sensor	Spatial resolution (m)	Path/Row	Use
01-28-2006	Landsat TM	30	232/083	cross-correlation
02-13-2006	Landsat TM	30	232/083	cross-correlation
01-15-2007	Landsat TM	30	232/083	cross-correlation
03-01-2007	Landsat TM	30	232/083	cross-correlation
03-28-2010	Landsat TM	30	232/083	inventory check
03-28-2010	Landsat TM	30	232/084	inventory check
03-31-2011	Landsat TM	30	232/083	glacier mapping
03-31-2011	Landsat TM	30	232/084	glacier mapping
03-22-2008	ALOS PRISM	10	11502/4325	DEM extraction
03-31-2011	ALOS PRISM	10	27606/4320	DEM extraction
03-31-2011	ALOS PRISM	10	27606/4325	DEM extraction
03-31-2011	ALOS PRISM	10	27606/4330	DEM extraction
03-31-2011	ALOS PRISM	10	27606/4335	DEM extraction
03-31-2011	ALOS PRISM	10	27606/4340	DEM extraction
03-31-2011	ALOS PRISM	10	27606/4345	DEM extraction
03-31-2011	ALOS PRISM	10	27606/4350	DEM extraction
03-31-2011	ALOS PRISM	10	27606/4355	DEM extraction
04-17-2011	ALOS PRISM	10	27854/4315	DEM extraction
04-17-2011	ALOS PRISM	10	27854/4320	DEM extraction